

FREE VIBRATIONS OF A STIFFENED  
RECTANGULAR PLATE

---

A Thesis  
Presented to  
the Faculty of the College of Engineering  
University of Houston

---

In Partial Fulfillment  
of the Requirements of the Degree  
Master of Science in Mechanical Engineering

---

by  
Duane R. Sanders  
December, 1977

## ACKNOWLEDGEMENTS

The author would like to thank Dr. C. D. Michalopoulos, Associate Professor of Mechanical Engineering, for his advice, guidance and patience during the course of this thesis. Appreciation is also extended to Dr. G. Pincus, Professor and Chairman of Civil Engineering, and Dr. R. R. Nachlinger, Associate Professor of Mechanical Engineering, for serving as committee members.

FREE VIBRATIONS OF A STIFFENED  
RECTANGULAR PLATE

---

An Abstract

Presented to

the Faculty of the College of Engineering  
University of Houston

---

In Partial Fulfillment

of the Requirements of the Degree

Master of Science in Mechanical Engineering

---

by

Duane R. Sanders

December, 1977

ABSTRACT

Free vibration of a thin rectangular plate stiffened by an arbitrary number of stiffeners parallel to a pair of its edges and simply supported on all edges, is considered. The equation of motion for the stiffened plate is derived by considering the stiffeners as producing external line loadings on the plate. Dirac delta functions are used to discretely locate these external loadings at the stiffener locations in the equation of motion. Solutions of the equation of motion are obtained from a system of equations of order  $R \times R$ , where  $R$  is equal to the number of stiffeners. Results for the natural frequencies and associated mode shapes are given for square plates stiffened by one, two, three and ten stiffeners and rectangular plates with two stiffeners. In each case, various stiffener flexural rigidities and linear mass densities were considered.

## TABLE OF CONTENTS

	Page
ABSTRACT .....	v
LIST OF TABLES .....	vii
LIST OF FIGURES .....	viii
LIST OF SYMBOLS .....	x
Chapter	
I. INTRODUCTION .....	1
II. EQUATION OF MOTION FOR STIFFENED-PLATE .....	4
III. FREE VIBRATIONAL ANALYSIS OF A PLATE WITH R-STIFFENERS .....	7
A. Solution of the Equations of Motion .....	7
B. Numerical Method for Determining Natural Frequencies .....	13
C. Solution for the Normal Modes of Vibration .....	15
IV. NUMERICAL RESULTS AND DISCUSSION .....	16
V. CONCLUSIONS AND RECOMMENDATIONS .....	41
BIBLIOGRAPHY .....	42
APPENDIX A .....	43

## LIST OF TABLES

Table		Page
1	Fundamental frequencies as functions of number of terms in each series of equation (3.19) .....	17
2	Ordering of natural frequencies for a plate with one stiffener .....	18
3	Ordering of natural frequencies for a plate with two stiffeners .....	19
4	Ordering of natural frequencies for a plate with three stiffeners .....	20

## LIST OF FIGURES

Figure		Page
1	Geometry and coordinate system of stiffened-plate .....	4
2	Reactions between plate and stiffeners .....	5
3	Lowest (first) natural frequencies and mode shapes (at $x/a = 0.5$ ) for a square plate with one stiffener .....	24
4	Second lowest natural frequencies and mode shapes (at $x/a = 0.25$ ) for a square plate with one stiffener .....	25
5	Third lowest natural frequencies and mode shapes (at $x/a = 0.5$ ) for a square plate with one stiffener .....	26
6	Lowest (first) natural frequencies and mode shapes (at $x/a = 0.5$ ) for a square plate with two stiffeners .....	27
7	Second lowest natural frequencies and mode shapes (at $x/a = 0.5$ ) for a square plate with two stiffeners .....	28
8	Third lowest natural frequencies and mode shapes (at $x/a = 0.25$ ) for a square plate with two stiffeners .....	29
9	Lowest (first) natural frequencies and mode shapes (at $x/a = 0.5$ ) for a square plate with three stiffeners .....	30
10	Second lowest natural frequencies and mode shapes (at $x/a = 0.5$ ) for a square plate with three stiffeners .....	31
11	Lowest (first) natural frequency and mode shapes (at $x/a = 0.5$ ) for a square plate with ten stiffeners .....	32
12	Finite element model for a square plate with one stiffener .....	33

Figure	Page
13	Comparison of lowest (first) natural frequency and mode shape of Fig. (3) with finite element solution ..... 34
14	Comparison of second lowest natural frequency and mode shape of Fig. (4) with finite element solution ..... 35
15	Finite element model for a square plate with two stiffeners ..... 36
16	Comparison of lowest (first) natural frequencies and mode shapes Fig. (6) with finite element solutions ..... 37
17	Comparison of lowest (third) natural frequencies and mode shapes Fig. (8) with finite element solution ..... 38
18	Lowest (first) natural frequencies and mode shapes (at $x/a = 0.5$ ) for a rectangular plate ( $a = 48$ in., $b = 24$ in.) with two stiffeners ..... 39
19	Lowest (first) natural frequencies and mode shapes (at $x/a = 0.5$ ) for a rectangular plate ( $a = 24$ in., $b = 48$ in.) with finite element solution ..... 40

## LIST OF SYMBOLS

$a$	= Dimension of plate in x-direction
$b$	= Dimension of plate in y-direction
$c_r$	= Distance to the rth stiffener, measured in the y-direction
$D$	= Flexural rigidity of plate, $Eh^3 / 12 (1 - \nu^2)$
$E$	= Young's modulus
$(EI)_r$	= Bending stiffness of rth stiffener
$I$	= Area moment of Inertia about y-axis
$h$	= Plate thickness
$h_b$	= Height of rectangular stiffener
$m$	= Number of half sine waves in x-direction
$n$	= Number of half sine waves in y-direction
$N$	= Number of terms retained in the Finite sine transform of Eq. (3.11)
$P_1(x)$	= Force per unit length on the plate due to the stiffener
$P_2(x)$	= Force per unit length on the stiffener due to the plate
$R$	= Number of stiffeners
$t$	= Time
$w(x, y, t)$	= $w(x, y) F(t)$ = Deflection of stiffened plate in z-direction as function of spatial coordinate and time
$x, y, z$	= Rectangular coordinates
$Y$	= Mode shape in y-direction
$\nabla^4$	= $(\frac{\partial}{\partial x^4} + 2 \frac{\partial}{\partial x^2} \frac{\partial}{\partial y^2} + \frac{\partial}{\partial y^4})$ = Biharmonic operator
$\delta$	= Dirac delta function

- $\nu$  = Poisson's ratio = 0.3
- $(\omega)_m$  = mth Natural frequency of stiffener (simply supported)
- $\omega_{mn}$  = Natural frequency of plate without stiffeners (simply supported)
- $\Omega_i$  = Natural frequencies of vibration obtained from Eq. (3.20)
- $\rho_s$  = Linear mass density of stiffener
- $\rho_p$  = Mass per unit area of plate
- { } = Indicates a column vector
- [ ] = Indicates a square matrix

## CHAPTER I

### INTRODUCTION

There are many applications where a stiffened plate proves to be the most economical arrangement of the structural material. Examples of this are found in aircraft and ship design where stiffened plates are used extensively. The ability to predict the natural frequencies and mode shapes of these stiffened plates is an important design aspect. For example in the design of a stiffened panel against flutter the determination of the natural frequencies of the stiffened panel is a necessary part of the analysis.

Previous free vibration analyses of a stiffened plate treat the plate-stiffener combination as an equivalent orthotropic plate [1, 2].<sup>1</sup> This procedure requires the determination of four rigidity constants which are used in the theory of thin orthotropic plates [3, 4]. Once these rigidity constants are known the natural frequencies and mode shapes are determined from the same mathematical procedure as an unstiffened plate. However, this type of analysis is limited to evenly and closely-spaced stiffeners and, therefore, the results are not applicable to sparsely-spaced stiffened plates.

To the best of the writer's knowledge, only one paper [5] was found in the literature in which the natural frequencies and mode shapes of a rectangular plate with sparsely-spaced stiffeners were

---

1. The number in brackets indicate reference at the end of thesis.

investigated. The stiffened plate analyzed was simply supported along two edges with the stiffeners being perpendicular to those two edges. In this method, first the free-vibrations solution is obtained for a panel supported simply on two parallel edges and by stiffeners along the other two edges. Then, a solution is constructed for a plate stiffened by any number of parallel stiffeners by imposing the compatibility of deflections and slopes at adjacent panels.

An alternate approach to that described in reference [5], which is employed herein, is to treat the effect of the stiffener as a load on the plate. This loading, which is assumed to be a line loading at the location of a stiffener, is introduced in the differential equation of motion by means of a Dirac delta function. This method has been successively applied in reference [6] to determine the critical buckling load of a sparsely-stiffened plate simply supported along the two of its edges which are perpendicular to the stiffeners. Another application of Dirac delta functions was given in reference [7]. There, the preload and weight distribution of a cable array embedded in a rectangular membrane was discretely loaded by Dirac delta functions. The resulting equation of motion was solved for the vibrational characteristics of the cable array embedded in the membrane.

In this thesis, the natural frequencies and associated mode shapes are determined for a simply supported, thin rectangular plate reinforced by an arbitrary number of sparsely-spaced

stiffeners parallel to a pair of its edges. The stiffeners are not necessarily evenly spaced nor do they have identical section properties. The stiffeners are assumed to conform to Euler-Bernoulli bending theory.

The differential equation of motion for a stiffened plate is derived in Chapter II. In Chapter III a closed form solution of the equation of motion for the natural frequencies and mode shapes is given. Also, the numerical procedures for determining the natural procedure for a plate with R-stiffeners and the associated deflections at the stiffener are described. Numerical results for the frequencies and the associated mode shapes are presented and discussed in Chapter IV. Finally, conclusions and recommendations are given in Chapter V.

CHAPTER II

EQUATION OF MOTION FOR A STIFFENED-PLATE

The equation of motion for a thin rectangular plate reinforced by an arbitrary number of stiffeners parallel to the x-axis (as shown in Figure 1) is derived in a manner similar to [8]. The usual assumptions of thin plate theory are made [4]. The only effect of the stiffeners on the plate considered is a loading along the line of contact between stiffener and plate in the transverse direction. This loading is due to both the bending resistance of the stiffener as well as its inertia.

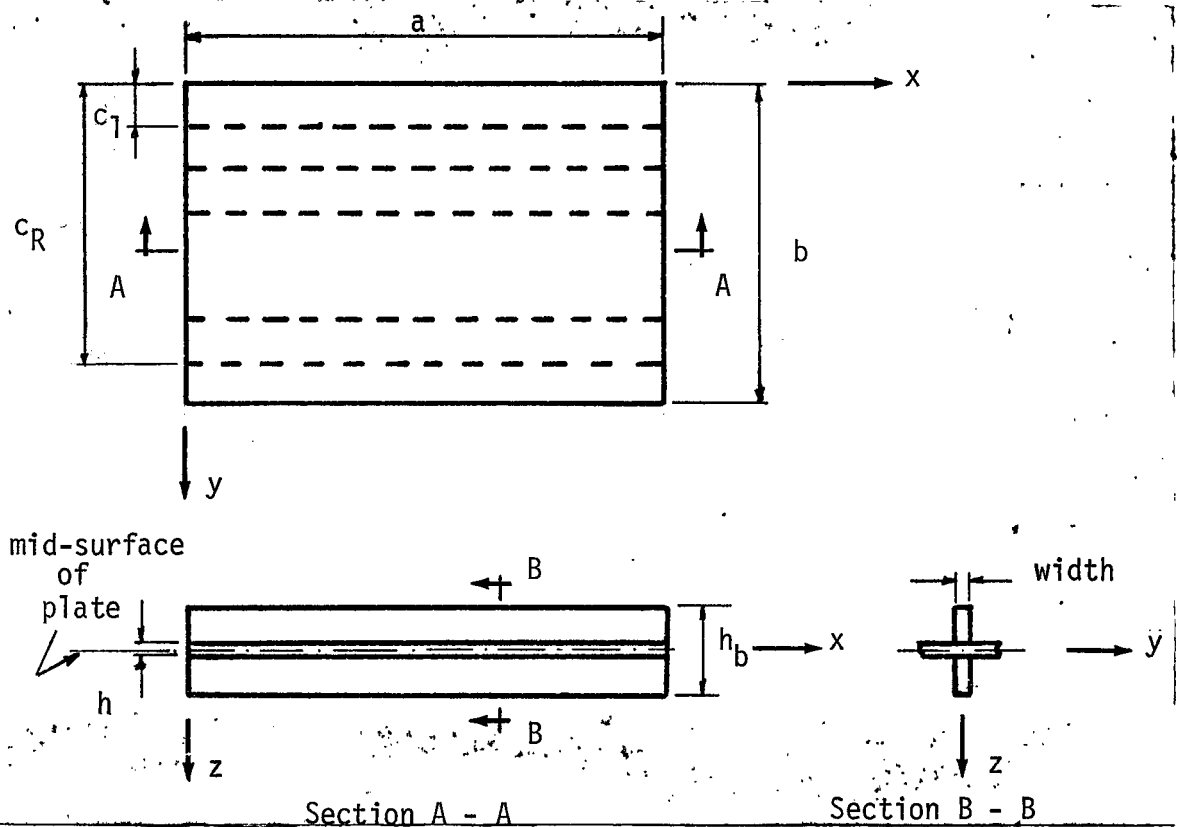


Figure 1. Geometry and Coordinate System of Stiffened-Plate.

It is noted that Figure 1 shows a rectangular reinforcement, but the analysis is equally applicable to other reinforcement shapes (e.g. I beams) which are located symmetrically about the mid-surface of the plate and whose centroid and shear center coincide. The stiffeners are assumed to conform to Euler-Berhoully beam theory. Thus, the force per unit length on the beam due to the plate is given by

$$P_1(x,t) = EI \frac{\partial^4 w}{\partial x^4} + \rho \frac{\partial^2 w}{\partial t^2} \quad (2.1)$$

The loading on the plate  $P_2(x,t)$ , is equal in magnitude but opposite in direction to  $P_1(x,t)$ , as shown in Figure 2.

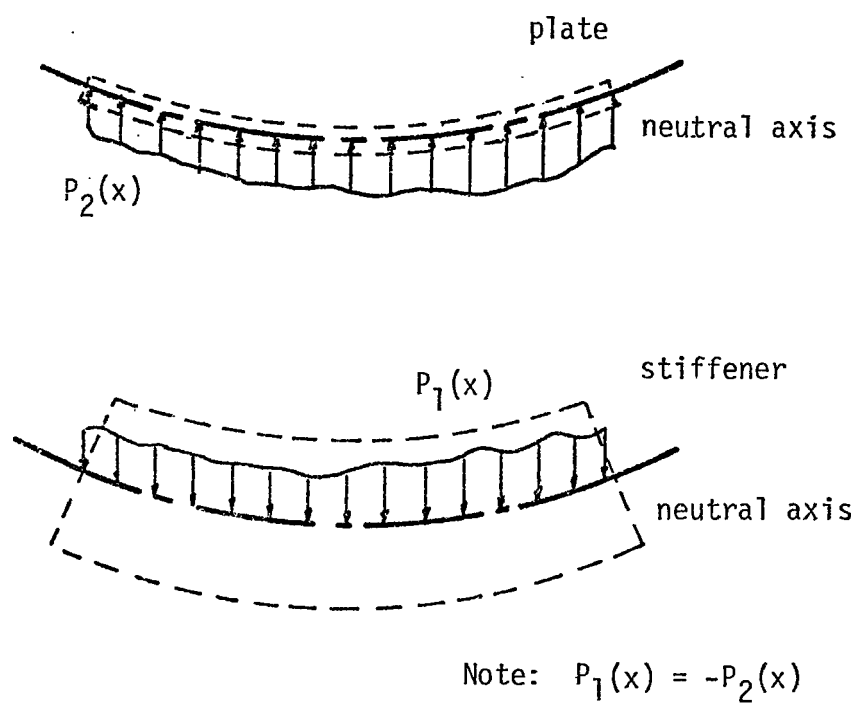


Figure 2. Reaction Between Plate and Stiffener.

The equations of motion for the plate-stiffener combination can be written considering the stiffeners as producing external loads on the plate given by (2.1). Dirac delta functions are used to discretize the loading on the plate along lines of contact between stiffener and plate. Therefore, the differential equation of motion for a plate with  $R$ -stiffeners parallel to the  $x$ -axis is

$$D\nabla^4 w = - \sum_{i=1}^R \left[ (EI)_i \frac{d^4 w}{dx^4} + (\rho_s)_i \frac{d^2 w}{dt^2} \right] \delta(y - c_i) \quad (2.2)$$

$$+ \rho_p \frac{\partial^2 w}{\partial t^2}$$

or,

$$D\nabla^4 w + \sum_{i=1}^R \left[ (EI)_i \frac{\partial^4 w}{\partial x^4} + (\rho_s)_i \frac{\partial^2 w}{\partial t^2} \right] \delta(y - c_i) \quad (2.3)$$

$$+ \rho_p \frac{\partial^2 w}{\partial t^2} = 0$$

It is seen that (2.3) is the familiar equation for free vibration of a plate except for the additional terms due to the loading imposed by the stiffeners.

## CHAPTER III

### FREE VIBRATION OF A RECTANGULAR PLATE WITH R-STIFFENERS

#### A. Solution of the equation of motion

As in the classical case of uniform plate, assume solutions of (2.3) of the form

$$w(x,y,t) = W(x,y) F(t) = W(x,y) e^{i\Omega t} \quad (3.2)$$

where  $F(t)$  is a harmonic function of time and  $\Omega$  is the frequency of  $F(t)$ . Substitution of (3.2) into (2.3) leads to

$$D \nabla^4 W - \sum_{i=1}^R \left[ (EI)_i \frac{\partial^4 W}{\partial x^4} - (\rho_s)_i \Omega^2 W \right] \delta(y - c_i) - \rho_p \Omega^2 W = 0. \quad (3.3)$$

Assume now a product solution for  $W(x,y)$  as follows:

$$W(x, y) = Y(y)X(x) = Y(y) \sin \frac{m\pi x}{a} \quad (3.4)$$

The form of the solution is motivated by the fact that a plate and beam both of which are simply supported at  $x=0,a$  have mode shapes which are of the form  $\sin \frac{m\pi x}{a}$ . Substituting (3.4) into (3.3) yields

$$\frac{d^4 Y}{dy^4} - 2 \left( \frac{m\pi}{a} \right)^2 \frac{d^2 Y}{dy^2} + \left[ \left( \frac{m\pi}{a} \right)^4 - \rho_p \frac{\Omega^2}{D} \right] Y$$

(3.5)

$$+ \frac{1}{D} \sum_{j=1}^R \left[ (EI)_j \left( \frac{m\pi}{a} \right)^4 - (\rho_s)_j \Omega^2 \right] Y \delta(y - c_j) = 0 .$$

A solution of (3.5) is obtained below by Fourier Finite Sine transforms, subject to the following boundary conditions:

$$W = 0, \frac{d^2 W}{dx^2} = 0, \text{ along } x = 0, a$$

(3.6)

$$W = 0, \frac{d^2 W}{dy^2} = 0, \text{ along } y=0, b .$$

From (3.4) and the second of (3.6), it follows that

$$Y(0) = 0$$

(3.7)

$$Y(b) = 0$$

and

$$\left( \frac{d^2 Y}{dy^2} \right)_{y=0} = 0$$

(3.8)

$$\left( \frac{d^2 Y}{dy^2} \right)_{y=b} = 0 .$$



$$\bar{Y}(n) = -\frac{1}{D} \frac{\sum_{i=1}^R \left[ (EI)_i \left( \frac{m\pi}{a} \right)^4 - (\rho_s)_i \Omega^2 \right] Y(c_i) \sin \frac{n\pi c_i}{b}}{\left[ \left( \frac{m\pi}{a} \right)^2 + \left( \frac{n\pi}{b} \right)^2 \right]^2 - \frac{\rho_p \Omega^2}{D}} \quad (3.11)$$

Taking the inverse transform of (3.11), gives for the function  $Y(y)$ :

$$Y(y) = -\frac{2}{bD} \sum_{n=1}^{\infty} \left\{ \frac{\sum_{i=1}^R \left[ (EI)_i \left( \frac{m\pi}{a} \right)^4 - (\rho_s)_i \Omega^2 \right] Y(c_i) \sin \frac{n\pi c_i}{a}}{\left[ \left( \frac{m\pi}{a} \right)^2 + \left( \frac{n\pi}{b} \right)^2 \right]^2 - \frac{\rho_p \Omega^2}{D}} \right\} \times \sin \frac{n\pi y}{b} \quad (3.12)$$

Introducing the expression for the natural frequency of a simply supported uniform plate,

$$\omega_{mn} = \left[ \left( \frac{m\pi}{a} \right)^2 + \left( \frac{n\pi}{b} \right)^2 \right] \sqrt{\frac{D}{\rho_p}} \quad (3.13)$$

and that for a uniform stiffener,

$$(\omega_m)_i = \left( \frac{EI}{\rho_s} \right)_i \left( \frac{m\pi}{a} \right)^2 \quad ,$$

into (3.13) yields,

$$y(y) = \frac{-2\rho_s}{b\rho_p} \sum_{n=1}^{\infty} \frac{\sum_{i=1}^R B_{mi}(\Omega) Y(c_i) \sin \frac{n\pi c_i}{b}}{A_{mn}(\Omega)} \sin \frac{n\pi y}{b} \quad (3.14)$$

where,

$\rho_s$  = mass per unit length of stiffener,

$\rho_p$  = mass per unit area of plate,

$A_{mn} = \omega_{mn}^2 - \Omega^2$ , and

$B_{mi} = (\omega_m)_i^2 - \Omega^2$ .

Set  $y = c_r$  in (3.14) where  $c_r$  is the  $y$  coordinate of the  $r$ th stiffener. Substituting and rearranging the following equation is obtained,

$$Y(c_r) \left[ 1 + \frac{2\rho_s}{b\rho_p} \sum_{n=1}^{\infty} \frac{B_{mr}(\Omega) \sin^2 \frac{n\pi c_r}{b}}{A_{mn}(\Omega)} \right] \quad (3.15)$$

$$+ \frac{2\rho_s}{b\rho_p} \left[ \sum_{n=1}^{\infty} \left\{ \sum_{i=1}^{r-1} \frac{B_{mi}(\Omega) \sin \frac{n\pi c_i}{b}}{A_{mn}(\Omega)} \sin \frac{n\pi c_r}{b} \right. \right.$$

$$\left. \left. + \sum_{i=r+1}^R \frac{B_{mi}(\Omega) \sin \frac{n\pi c_i}{b} \sin \frac{n\pi c_r}{b}}{A_{mn}(\Omega)} \right\} \right] = 0.$$

Equation (3.15) can be rewritten as

$$Y(c_r)[1 + Z_{ir}^{mn}(\Omega)] + \sum_{i=1}^{r-1} Z_{ir}^{mn} Y(c_i) + \sum_{i=r+1}^R Z_{ir}^{mn} Y(c_i) = 0 \quad (3.16)$$

where,

$$Z_{ir}^{mn}(\Omega) = \frac{2 \rho_s}{b \rho_p} \sum_{n=1}^{\infty} \frac{B_{mi}(\Omega) \sin \frac{n\pi c_i}{b} \sin \frac{n\pi c_r}{b}}{A_{mn}(\Omega)} \quad (3.17)$$

For a plate with R-stiffeners, the following system of R equations is obtained by imposing condition (3.16) for each of the stiffeners,

$$\begin{bmatrix} 1 + Z_{11}^{mn}(\Omega) & Z_{21}^{mn}(\Omega) & Z_{31}^{mn}(\Omega) & \dots & Z_{R1}^{mn}(\Omega) \\ Z_{12}^{mn}(\Omega) & 1 + Z_{22}^{mn}(\Omega) & Z_{32}^{mn}(\Omega) & \dots & Z_{R2}^{mn}(\Omega) \\ Z_{13}^{mn}(\Omega) & Z_{23}^{mn}(\Omega) & 1 + Z_{33}^{mn}(\Omega) & \dots & Z_{R3}^{mn}(\Omega) \\ \cdot & \cdot & \cdot & \dots & \cdot \\ \cdot & \cdot & \cdot & \dots & \cdot \\ \cdot & \cdot & \cdot & \dots & \cdot \\ \cdot & \cdot & \cdot & \dots & \cdot \\ Z_{1R}^{mn}(\Omega) & Z_{2R}^{mn}(\Omega) & Z_{3R}^{mn}(\Omega) & \dots & 1 + Z_{RR}^{mn}(\Omega) \end{bmatrix} \begin{Bmatrix} Y(c_1) \\ Y(c_2) \\ Y(c_3) \\ \cdot \\ \cdot \\ \cdot \\ \cdot \\ Y(c_R) \end{Bmatrix} = \{0\} \quad (3.18)$$

or,

$$[Z(\Omega)] \{Y\} = 0 \quad (3.19)$$

The above system of equations has a non-trivial solution if and only if the determinant of the matrix of coefficients is equal to zero.

Therefore, the natural frequencies of a plate with R-stiffeners are those frequencies that satisfy the frequency equation,

$$\det ([Z]) = 0 \quad (3.20)$$

It should be pointed out that (3.20) does not yield all natural frequencies, since the trivial solution of (3.18), namely  $Y(c_i) = 0$ ,  $i=1, 2, \dots, R$ , is not included. This corresponds to the case for which all stiffeners lie along nodal lines of the unstiffened plate, i.e. their deflection is zero. The frequencies of such modes are determined from the classical expression as given previously by equation (3.13). Hence in order to determine successive natural frequencies of a plate reinforced by R-stiffeners it is necessary to consider both the frequencies corresponding to mode shapes with non-zero displacements and those with zero displacements at the stiffeners.

#### B. Numerical Procedure for Determining the Natural Frequencies

Due to the nature of equations (3.17) and (3.18), it is quite tedious to expand the determinant of (3.20) and obtain an equation of the form

$$\Omega^n + \alpha_1 \Omega^{n-1} + \alpha_2 \Omega^{n-2} + \dots + \alpha_n = 0 \quad (3.21)$$

This is true even in the case of a single stiffener.

In view of the above, the natural frequencies were determined approximately by the following procedure: First, the frequency is incremented until two successive values are found for which the determinant of (3.20) changes sign. This indicates that a root of (3.20) has been isolated. To expand the determinant for any value of the frequency the method of pivotal condensation is used. This method was chosen due to the ease with which it can be programmed. The method is described in detail in reference [10].

Once a root has been isolated by the above search process, the values of the successive frequencies and the corresponding values of the determinant are used in a modified false-position method to obtain the root in question to any desired degree of accuracy. The method of modified false position is described in detail in [9].

It should be noted that the value of a given root as well as the number of roots that can be determined depend on the number of terms in the series which are involved in the elements of the determinant of (3.20). When  $N$  terms of the series are retained the lowest  $N$  natural frequencies are determined. If  $N + 1$  terms are used, the accuracy for the first  $N$  frequencies is improved and a first estimate of the  $N + 1$  frequency is obtained, as in the Rayleigh-Ritz method.

### C. Numerical Solution Procedure for Normal Modes of Vibration

Consider the set of homogeneous algebraic equations (3.18). For a natural frequency, the coefficient matrix is completely determined. We need to determine what values of  $Y(c_1)$ ,  $Y(c_2)$ ,  $Y(c_3)$ , ...  $Y(c_R)$  satisfy these equations. We know that the  $R \times R$  determinant of (3.20) is, at most, of rank  $R-1$ . From matrix theory, if a homogeneous system of  $R$  equations  $[Z] \{Y\} = 0$  is of rank  $R-1$  and the submatrix obtained from  $[Z]$  by omitting the  $k^{\text{th}}$  row is also of order  $R-1$ , then a complete solution of the given system of equations is

$$Y_i = \beta Z_{ki} \quad i = 1, 2, \dots, R$$

where  $\beta$  is an arbitrary constant, and  $Z_{ki}$  is a cofactor of  $[Z]$ .

In the results presented in Chapter IV the arbitrary constants are selected such that the maximum modal displacement of the plate is equal to one.

CHAPTER IV  
NUMERICAL RESULTS AND DISCUSSION

A computer program was written to perform the numerical calculations outlined in Chapter III for determining the natural frequencies and associated mode shapes for a stiffened plate. This program calculates only those frequencies and associated mode shapes whose displacement at the stiffeners are not all zero. This program is included as Appendix A.

The natural frequencies and the associated mode shapes were obtained, for non-zero displacements at the stiffeners, for the following cases:

- (i) Square plate ( $a = 48$  in.,  $b = 48$  in.) with simply supported edges for one stiffener of various section properties ( $\rho_s, I$ ) evenly spaced across the plate in the  $y$ -direction and parallel to the  $x$ -axis.
- (ii), (iii) and (iv) are identical to (i) but for two, three, and ten stiffeners, respectively.
- (v) Rectangular geometry ( $a = 48$  in.,  $b = 24$  in.) with two stiffeners of various section properties ( $I, \rho_s$ ) evenly spaced across the plate in the  $y$ -direction and parallel to the  $x$ -axis.
- (vi) Same as (v), except ( $a = 24$  in. and  $b = 48$  in.).

For all cases considered above, the thickness of the plate was 0.25 inches and the sections properties were determined for a rectangular stiffeners of width  $\frac{1}{2}$  inch.

In the determinant of equation (3.20) each term involves a summation of infinitely many terms. Table 1 gives the lowest natural

frequencies and percent change (in these frequencies) as more terms are retained in (3.20) for one, two and three stiffeners. All stiffeners were considered to have a  $I = 1.0 \text{ in.}^4$  and  $\rho_s = 0.00157 \text{ slugs/in.}$  It is seen from Table 1 that in all cases the percent change between  $N = 20$  and  $N = 30$  terms is less than 0.01 percent. Thirty terms ( $N = 30$ ) were used throughout this thesis.

Table 1. Fundamental Frequencies as Functions of Number of Terms in Series of Equation (3.20)

No. of terms retained N	1 stiffener		2 stiffener		3 stiffener	
	$\Omega \left(\frac{\text{rad}}{\text{sec}}\right)$	% $\Delta\Omega$	$\Omega \left(\frac{\text{rad}}{\text{sec}}\right)$	% $\Delta\Omega$	$\Omega \left(\frac{\text{rad}}{\text{sec}}\right)$	% $\Delta\Omega$
1	321.58		368.39		417.98	
5	290.56	9.65	362.69	1.54	411.79	1.48
10	289.58	0.33	361.23	0.40	410.63	0.28
20	289.33	0.086	360.79	0.12	410.35	0.08
30	289.31	0.007	360.77	0.006	410.32	0.007

Table 2 gives the ordering of the natural frequencies for Case (i). The associated mode shapes are shown in Figs. 3, 4 and 5 for those frequencies obtained from Eq. (3.20), i.e. for the non-trivial solution. The natural frequencies for the modes with zero stiffener displacement were obtained using Eq. (3.13) for a simply supported square plate. Note that  $n$  (number of half sine waves in  $y$ -direction) must be an even number to have zero displacements at the stiffener.

Table 2. Ordering of Natural Frequencies for a Plate With One Stiffener

Order of Natural Frequencies	$I = 1.0 \text{ in.}^4$	$I = 3.75 \text{ in.}^4$	$I = 10.0 \text{ in.}^4$
	$\Omega, \omega \text{ (rad/sec)}$	$\Omega, \omega \text{ (rad/sec)}$	$\Omega, \omega \text{ (rad/sec)}$
1st	$\Omega_1 = 289.5$	$\omega_{12} = 312.1$	$\omega_{12} = 312.1$
2nd	$\omega_{12} = 312.1$	$\Omega_1 = 385.9$	$\Omega_1 = 418.4$
3rd	$\omega_{22} = 499.4$	$\omega_{22} = 499.4$	$\omega_{22} = 499.4$
4th	$\Omega_2 = 578.1$	$\Omega_2 = 788.0$	
5th	$\Omega_3 = 625.2$		

$\omega_{mn}$  = Natural frequencies corresponding to zero stiffener displacement as determined from Eq. (3.13).

$\Omega_i$  = Natural frequencies corresponding to non-zero stiffener displacement as determined from Eq. (3.20).

Table 3 gives the ordering of the natural frequencies for two stiffeners, Case (ii). The associated mode shapes are shown in Figs. 6, 7 and 8 for those frequencies obtained from equation (3.20). The natural frequencies for the modes with zero displacements at the stiffeners were obtained using Eq. (3.13). Note that  $n$  must be a multiple of three to have zero displacements at both stiffeners.

Table 3. Ordering of Natural Frequencies for a Plate With Two Stiffeners

Order of Natural Frequencies	$I = 1.0 \text{ in.}^4$	$I = 2.5 \text{ in.}^4$	$I = 3.75 \text{ in.}^4$	$I = 5.0 \text{ in.}^4$
	$\Omega, \omega$ (rad/sec)	$\Omega, \omega$ (rad/sec)	$\Omega, \omega$ (rad/sec)	$\Omega, \omega$ (rad/sec)
1st	$\Omega_1 = 361.0$	$\Omega_1 = 517.0$	$\Omega_1 = 600.5$	$\omega_{13} = 624.5$
2nd	$\Omega_2 = 440.2$	$\Omega_2 = 548.9$	$\Omega_2 = 603.5$	$\Omega_1 = 641.0$
3rd	$\omega_{13} = 624.3$	$\omega_{13} = 624.3$	$\omega_{23} = 624.5$	$\Omega_2 = 664.7$
4th	$\omega_{23} = 811.5$	$\omega_{23} = 811.5$	$\omega_{23} = 811.5$	$\omega_{23} = 811.5$
5th	$\Omega_3 = 893.2$	$\Omega_3 = 924.5$		

$\omega_{mn}$  = Natural frequencies corresponding to zero displacement at the stiffeners as determined from equation (3.13).

$\Omega_i$  = Natural frequencies corresponding to non-zero displacements at the stiffeners as determined from equation (3.20).

Table 4 gives the ordering of the natural frequencies for three stiffeners, Case (iii). The associated mode shapes are shown in Figs. 9 and 10 for those frequencies obtained from Eq. (3.20). The natural frequencies for the modes with zero displacements at the stiffeners were obtained from Eq. (3.13). Note that  $n$  must be a multiple of four to give zero displacements at the stiffeners.

Table 4. Ordering of Natural Frequencies for a Plate With Three Stiffeners.

Order of Natural Frequencies	$I = 1.0 \text{ in.}^4$	$I = 2.5 \text{ in.}^4$	$I = 5.0 \text{ in.}^4$
	$\Omega$ (rad/sec)	$\Omega$ (rad/sec)	$\Omega$ (rad/sec)
1st	$\Omega_1 = 401.7$	$\Omega_1 = 584.7$	$\Omega_1 = 773.5$
2nd	$\Omega_2 = 465.3$	$\Omega_2 = 753.4$	$\Omega_2 = 794.2$
3rd	$\Omega_3 = 641.3$		$\Omega_3 = 880.9$

$\omega_{mn}$  = Natural frequencies associated with zero-displacements at the 3 stiffeners as determined from equation (3.13).

$\Omega_i$  =  $i^{\text{th}}$  Natural frequency associated with non-zero displacements at the 3 stiffeners as determined from equation (3.20).

Since, the main interest in this study lies in the effect of the stiffeners on the free-vibration characteristics of the stiffened plate, the familiar modes corresponding to zero deflection at the stiffeners are not presented.

The following two observations can be made in general by studying the results in Figs. 3, 4, 5, 6, 7, 8, 9, 10, 11, 18 and 19 for the natural frequencies and associated mode shapes given in each of these figures. First, for the section properties considered, the effect of increasing the section properties of the stiffener (stiffeners) is to increase the natural frequencies of the stiffened plate. It should be noted that this result is not, in general true. In fact, if the mass per unit length ( $\rho_s$ ) of the stiffener were to increase faster than its bending stiffness, the natural frequencies decrease. Secondly, the figures for each of the cases considered (with

the exception of Figs. 6 and 7 for  $I = 5.0 \text{ in.}^4$ ) show that as the section properties are increased the mode shapes become more distorted and the modal displacements at the stiffeners are reduced. These results are as one would expect since the effect of a stiffener is equivalent to a line loading on the plate in a direction opposite to the displacement of the plate.

In Fig. 6 and 7 the mode shapes for the case  $I = 5.0 \text{ in.}^4$ ,  $\rho = 0.001807 \text{ slugs/in.}$  for the 1st and 2nd lowest frequency, respectively, indicate mode shapes which appear to be inconsistent with the others shown in each of these figures. It is shown in Fig. 16 by comparison with finite-element analysis that the modal shape given in Fig. 6 is indeed the correct mode shape for the 1st natural frequency associated with non-zero displacement at the two stiffeners. Although not shown in a figure, the mode shapes shown in Fig. 7 for  $I = 5.0 \text{ in.}^4$  was also verified.

Figure 11 shows a comparison between the lowest natural frequency and mode shape for a square plate with ten stiffeners determined by the method of this thesis and that of orthotropic plate theory. In this case the distance between the stiffeners is 4.36 inches. The natural frequency and mode shape obtained by these two methods show excellent agreement. The natural frequencies differ by only 2.58 percent.

Figure 18 shows the natural frequencies and associated mode shapes for the rectangular plate ( $a = 48 \text{ in.}$ ,  $b = 24.$ ) of Case (v). In this case, the two stiffeners are closer together in the y-direction than they were for Case (ii) above. It is noticed that the relatively

large change in section properties ( $I = 1.0 \text{ in.}^4$  to  $I = 10.0 \text{ in.}^4$ ) of Fig. 7 causes very little distortion of the mode shape compared to the distortion indicated in Fig. 6 for a smaller change in the properties ( $I = 1.0 \text{ in.}^4$  to  $I = 5.0 \text{ in.}^4$ ). This indicates that the rectangular stiffened plate is acting in a manner closer to that of an orthotropic plate.

Since no experimental results for the natural frequencies and associated mode shapes for a stiffened plate are available, the results of this study were compared to those obtained by means of a finite-element program (Strudl). This was done for one and two stiffeners. Figure 12 shows a finite-element model used for a plate with one stiffener. In this model, 72 plate bending elements and 6 beam elements were used. Figure 15 shows an 84 element model for a plate with two stiffeners. In this model 72 plate bending and 12 beam elements were used.

It should be noted that the plate bending element used in the above finite-element model is an incompatible finite-element. An element of this type does not converge from the high side as compatible elements do, as the mesh is refined. Instead, as the mesh is refined, this element converges from the low side.

Figure 13 shows a comparison of the lowest frequency and associated mode shape for a plate with one stiffener obtained from the finite-element program (Strudl) to that given in Fig. 3 for  $I = 1.0 \text{ in.}^4$ . The natural frequencies and mode shapes obtained by the two methods are in excellent agreement. The natural frequencies

differ by only 0.9 percent.

Figure 14 gives a similar comparison for the 2nd lowest natural frequency of a plate stiffened with one stiffener. The mode shapes shown for both solution techniques show good agreement, but the natural frequencies differ by 4.7 percent.

The author believes that a reduction in the mesh size for the finite-element model would bring the results for the second natural frequencies and associated mode shapes obtained by two methods into better agreement.

The results for two of the cases plotted in Fig. 6, namely,  $I = 1.0 \text{ in.}^4$ ,  $\rho = 0.001057 \text{ slugs/in.}$ ;  $I = 5.0 \text{ in.}^4$ ,  $\rho = 0.001807 \text{ slugs/in.}$ , are compared with the solution obtained from the finite-element program Strud1 (for the model of Fig. 15) in Fig. 16. The natural frequencies and mode shapes given by both solution techniques for  $I = 1.0 \text{ in.}^4$  show excellent agreement. The natural frequencies differing by only 0.58 percent. The mode shapes for  $I = 5.0 \text{ in.}^4$  also show good agreement, but the natural frequencies differ by 6.05 percent.

Figure 17 makes the same comparison as Fig. 16 except it is for the third lowest natural frequency. Again, the natural frequency and mode shape taken from Fig. 7 show excellent agreement with that predicted by the finite-element solution.

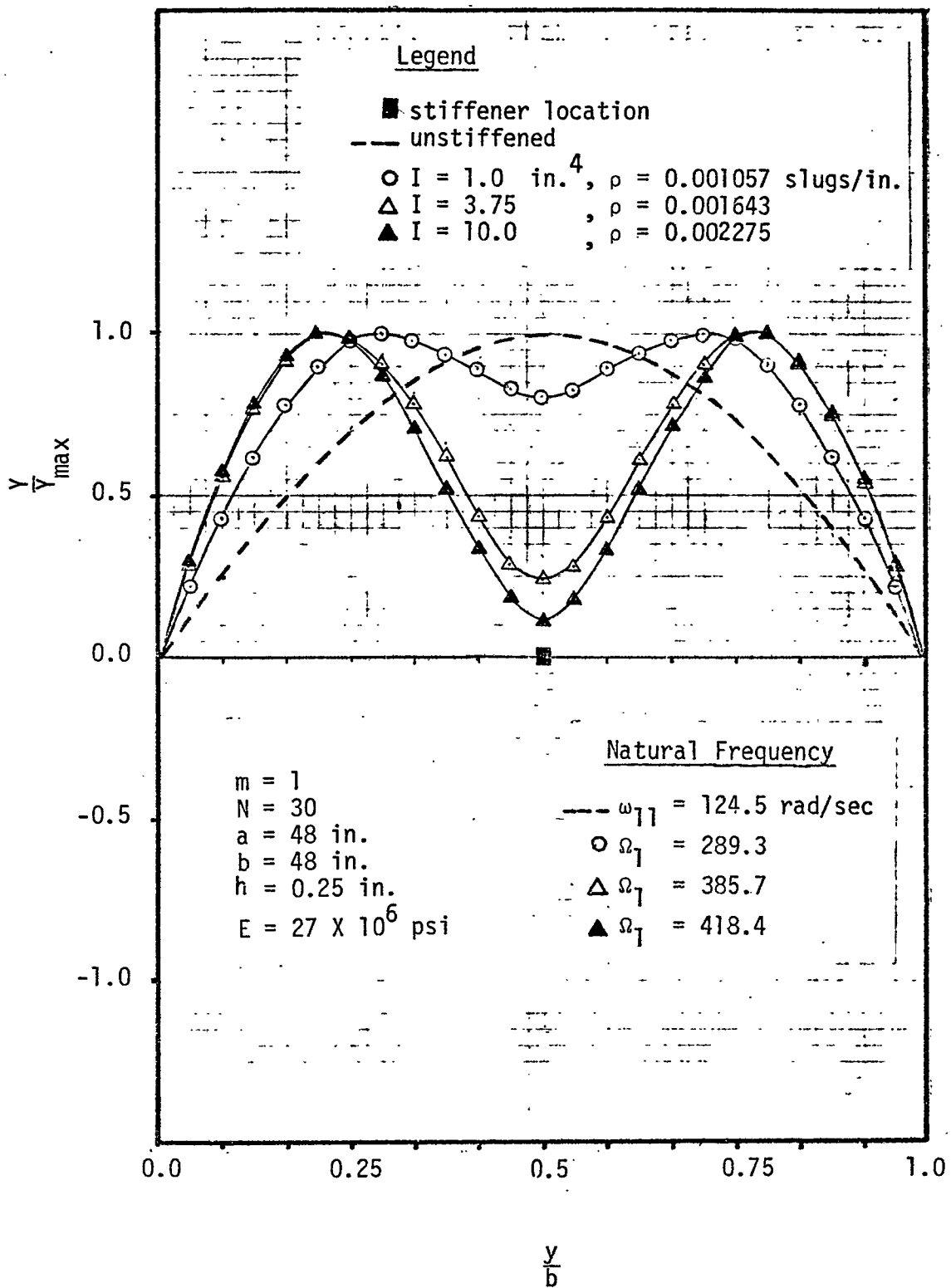


Fig. 3. Lowest (first) natural frequencies and mode shapes (at  $x/a = 0.5$ ) for a square plate with one stiffener.

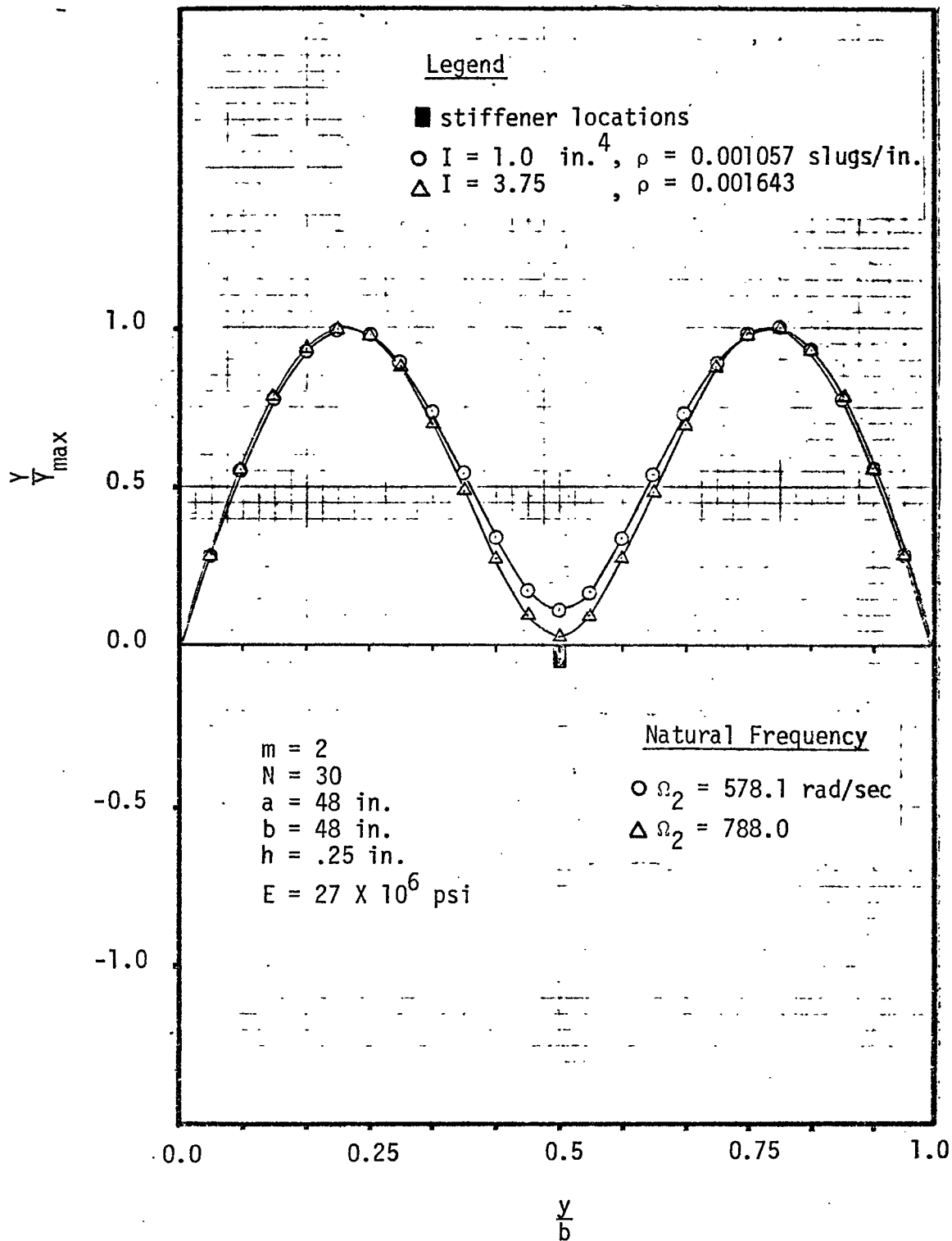


Fig. 4. Second lowest natural frequencies and mode shapes (at  $x/a = 0.25$ ) for a square plate with one stiffener.

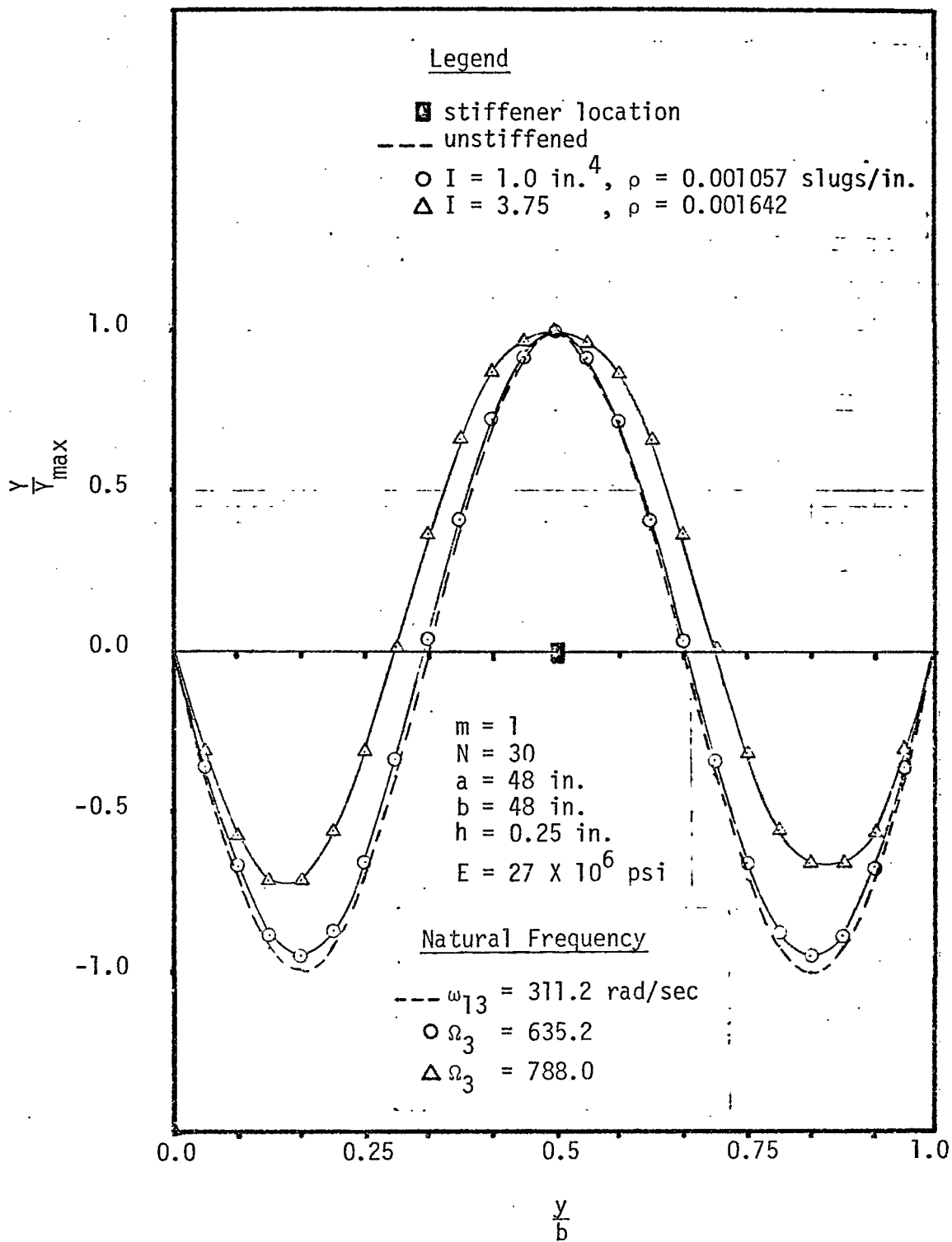


Fig. 5 Third lowest natural frequencies and mode shapes (at  $x/a = 0.5$ ) for a square plate with one stiffener.

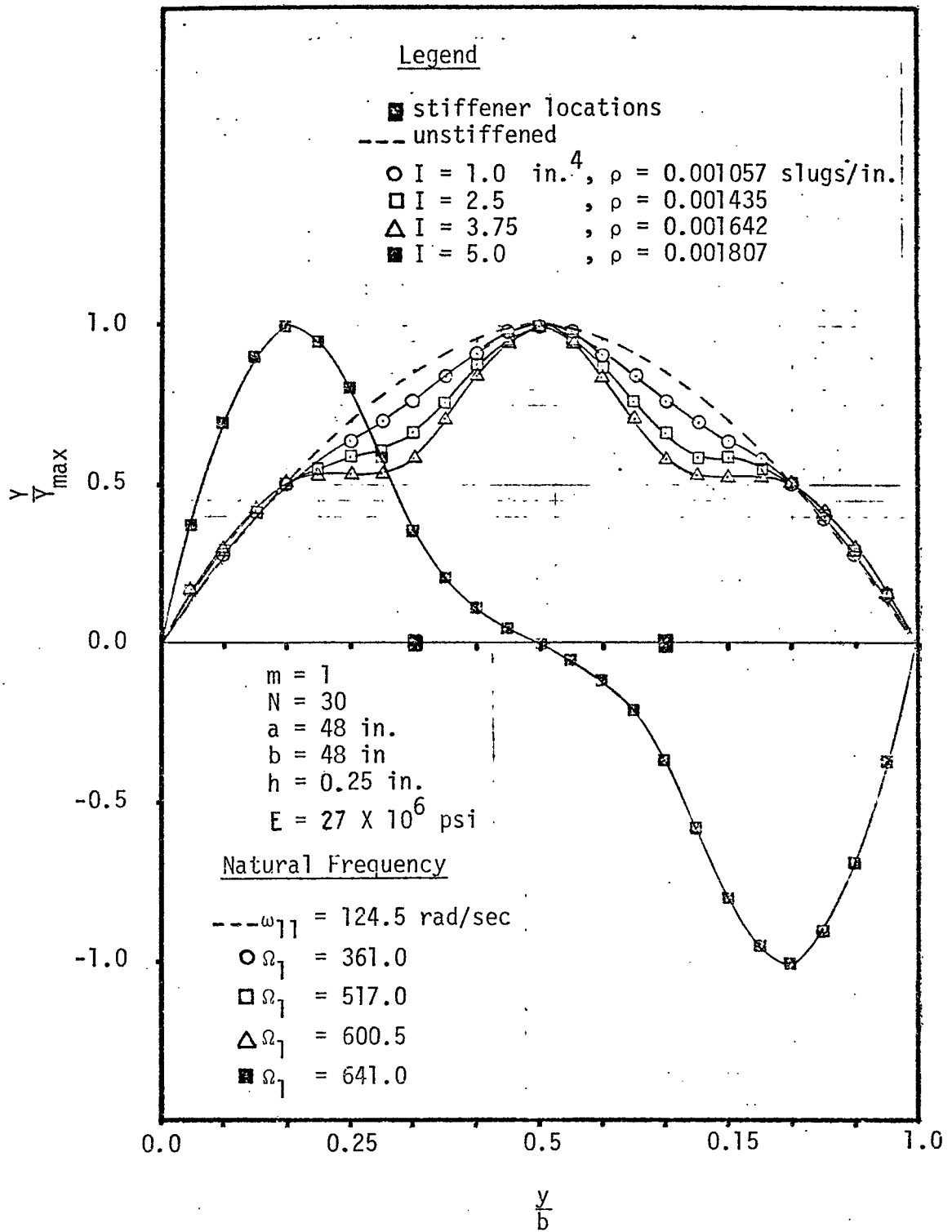


Fig. 6. Lowest (first) natural frequencies and mode shapes (at  $x/a = 0.5$ ) for a square plate with two stiffeners.

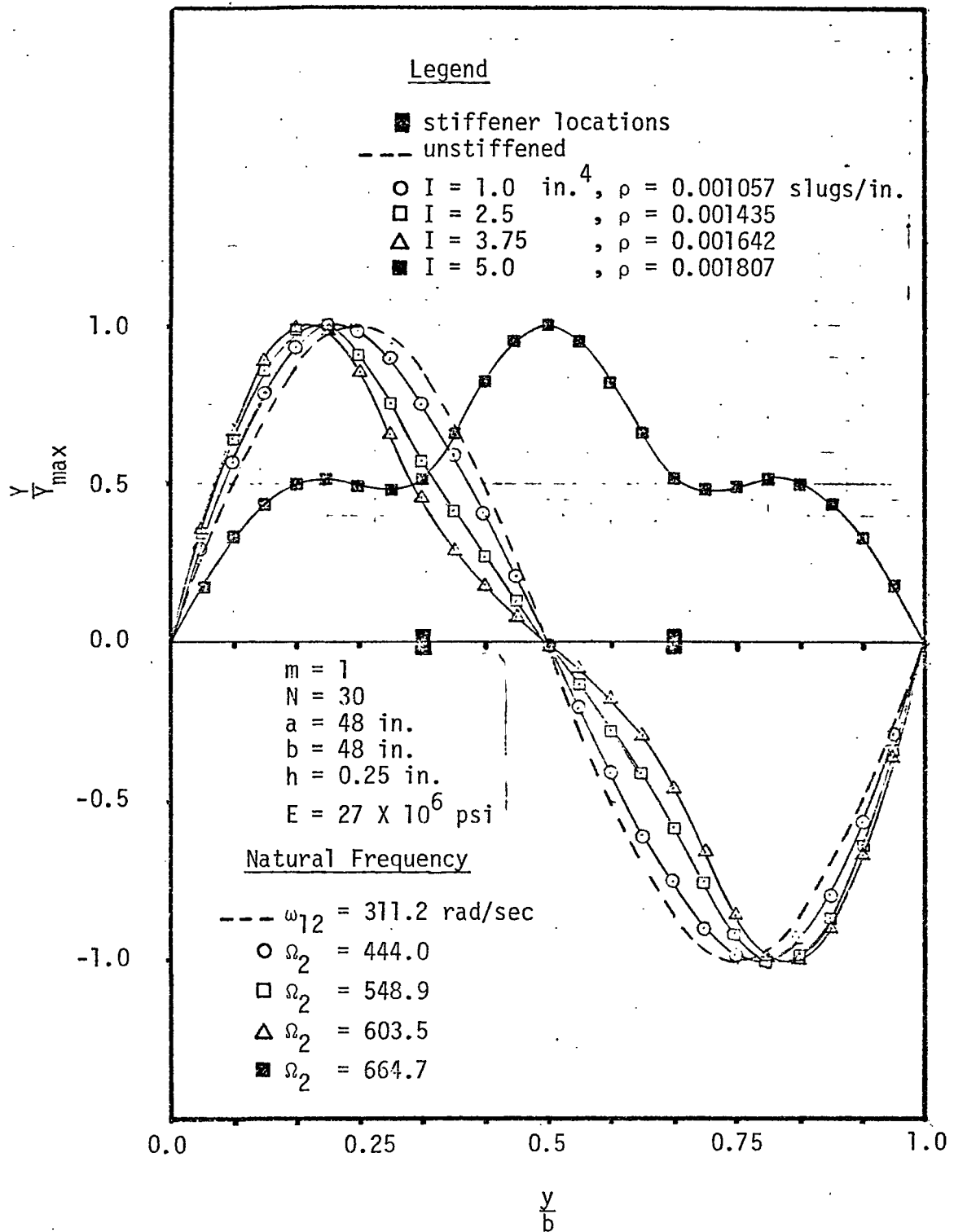


Fig. 7. Second lowest natural frequencies and mode shapes (at  $x/a = 0.5$ ) for a square plate with three stiffeners.

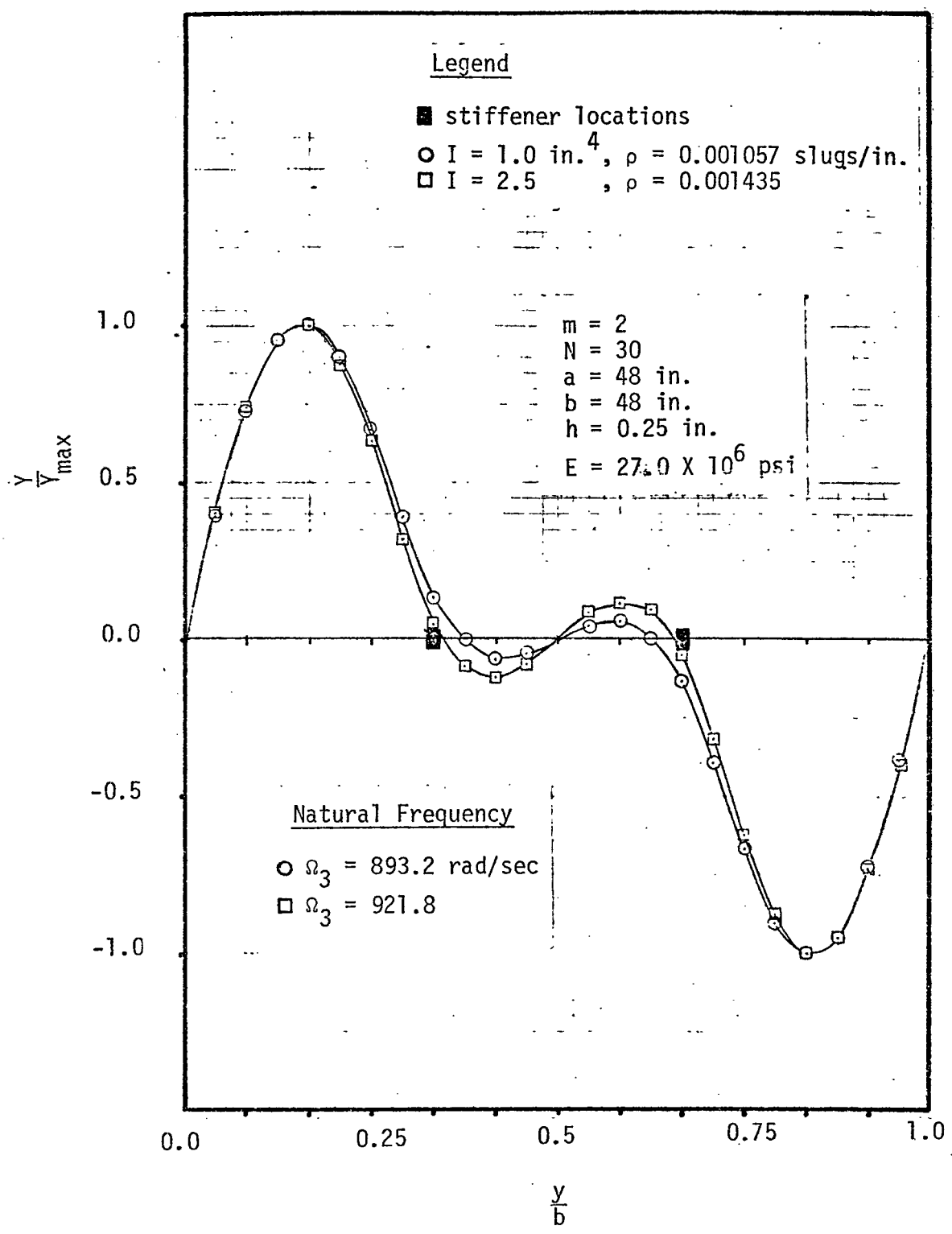


Fig. 8. Third lowest natural frequencies and mode shapes (at  $x/a = 0.25$ ) for a square plate with two stiffeners.

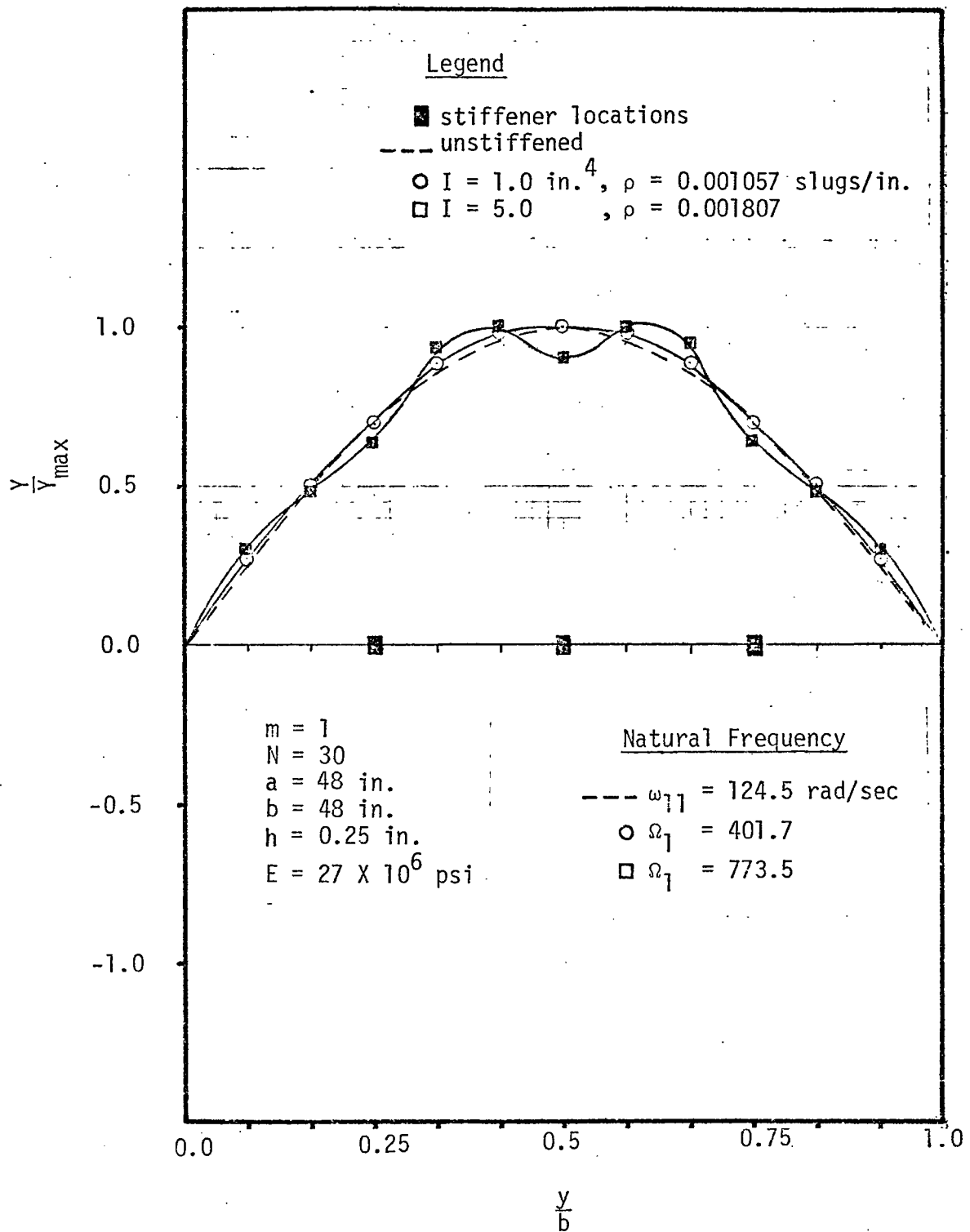


Fig. 9. Lowest (first) natural frequencies and mode shapes (at  $x/a = 0.5$ ) for a square plate with three stiffeners.

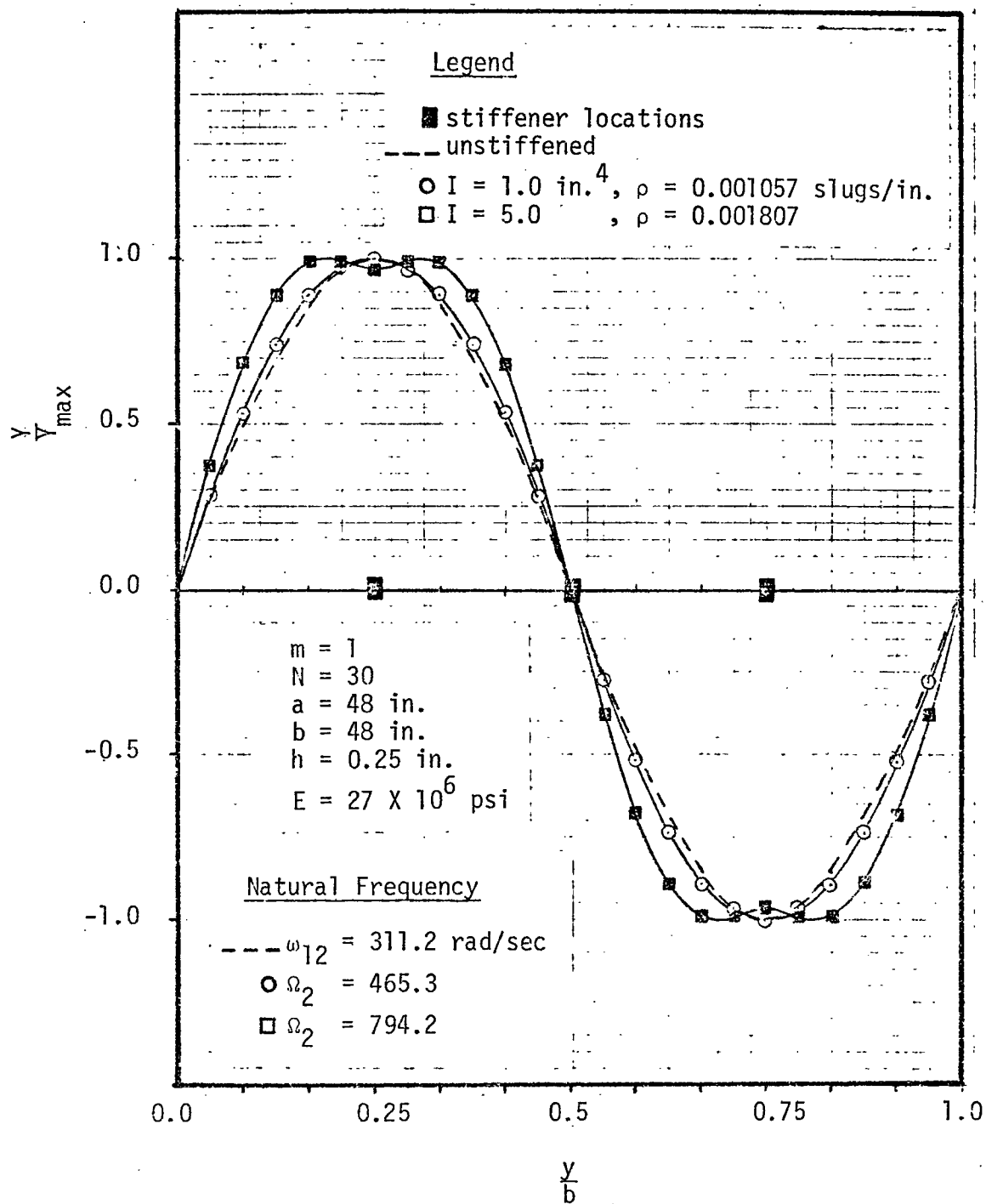


Fig. 10. Second lowest natural frequency and mode shapes (at  $x/a = 0.5$ ) for a square plate with three stiffeners.

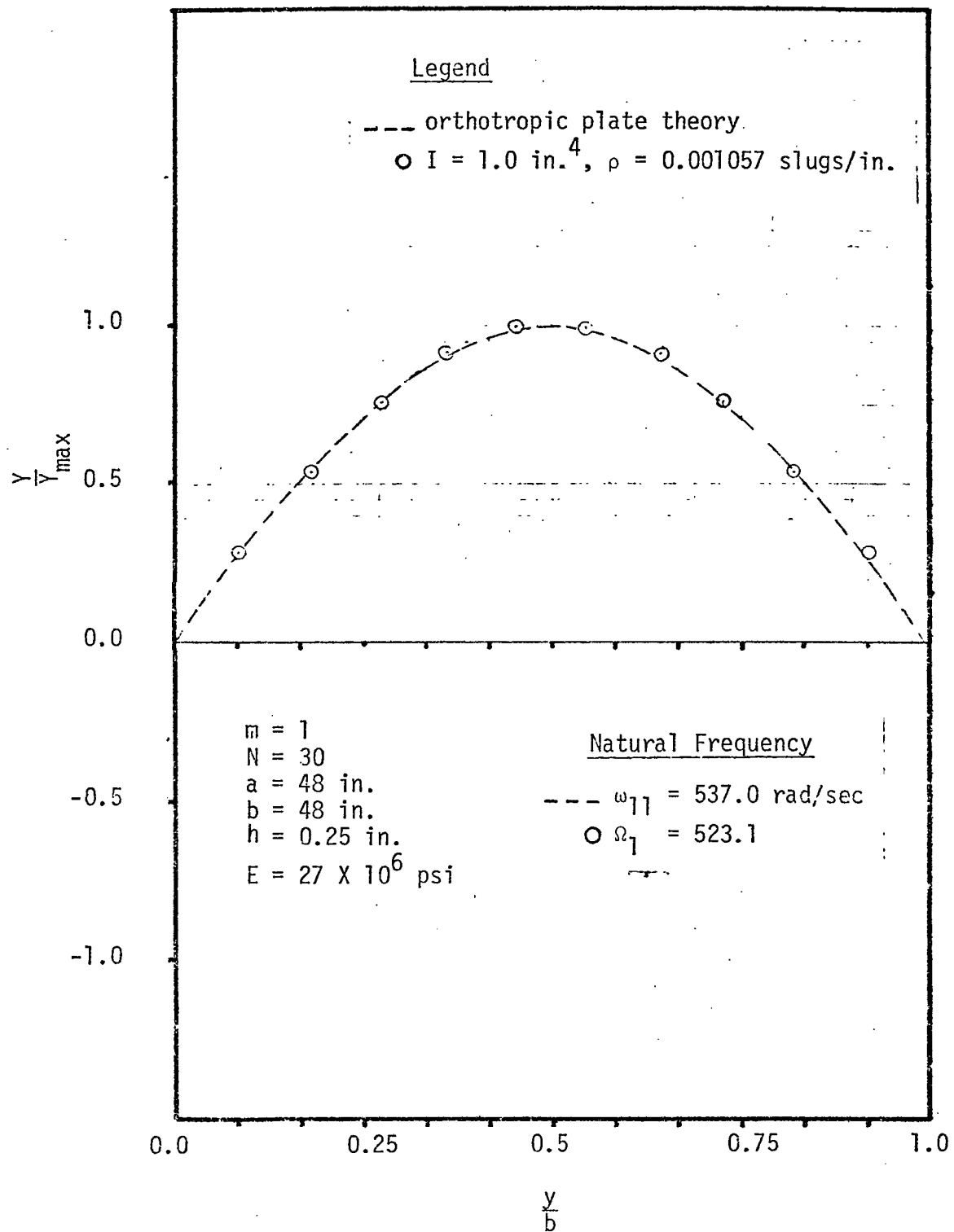
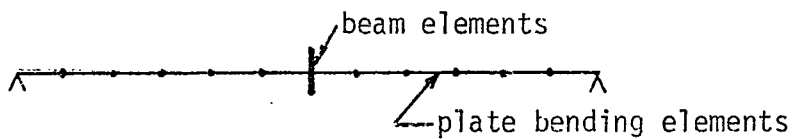
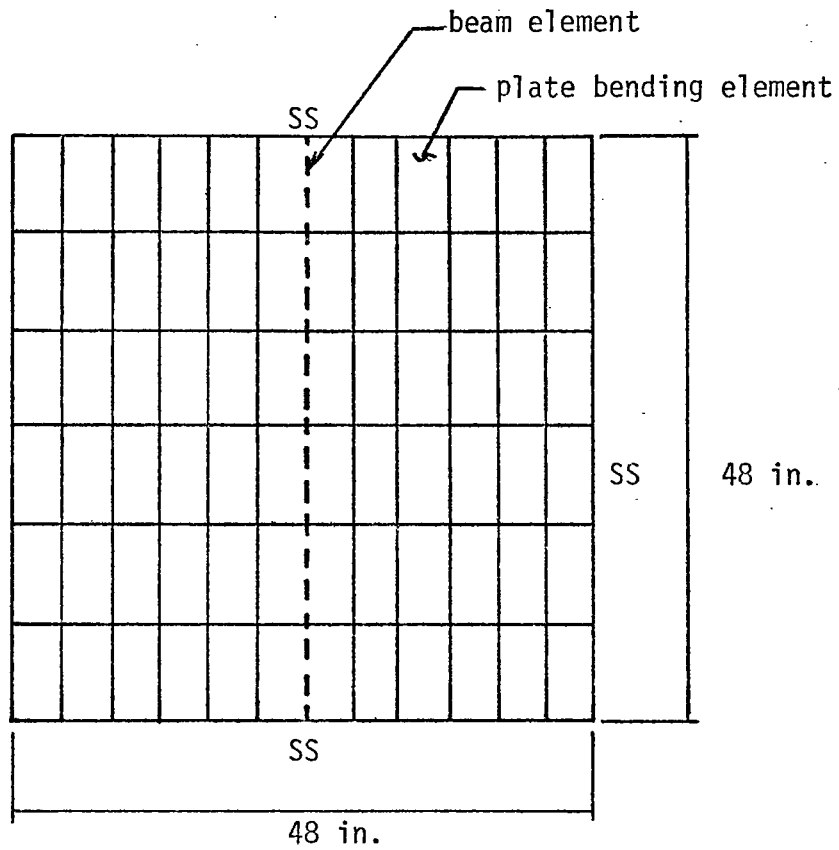


Fig. 11. Lowest (first) natural frequency and mode shapes (at  $x/a = 0.5$ ) for a square plate with ten stiffeners.



--- stiffener locations

SS: Simply supported

78 elements } 72 plate bending elements  
                   } 6 beam elements

Fig. 12. Finite-element model for a square plate with one stiffener.

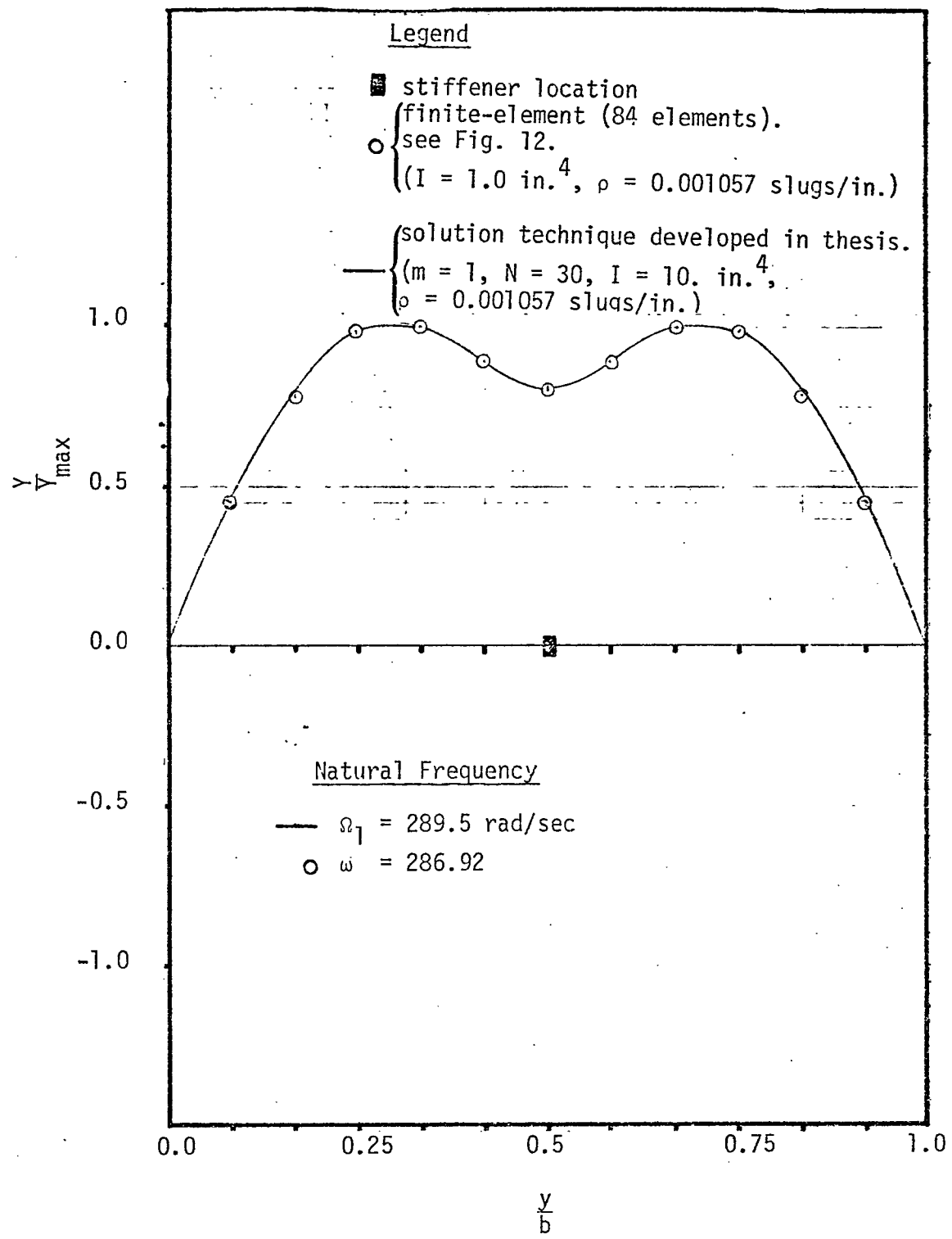


Fig. 13. Comparison of lowest (first) natural frequency and mode shapes of Fig. 3 with finite-element solution.

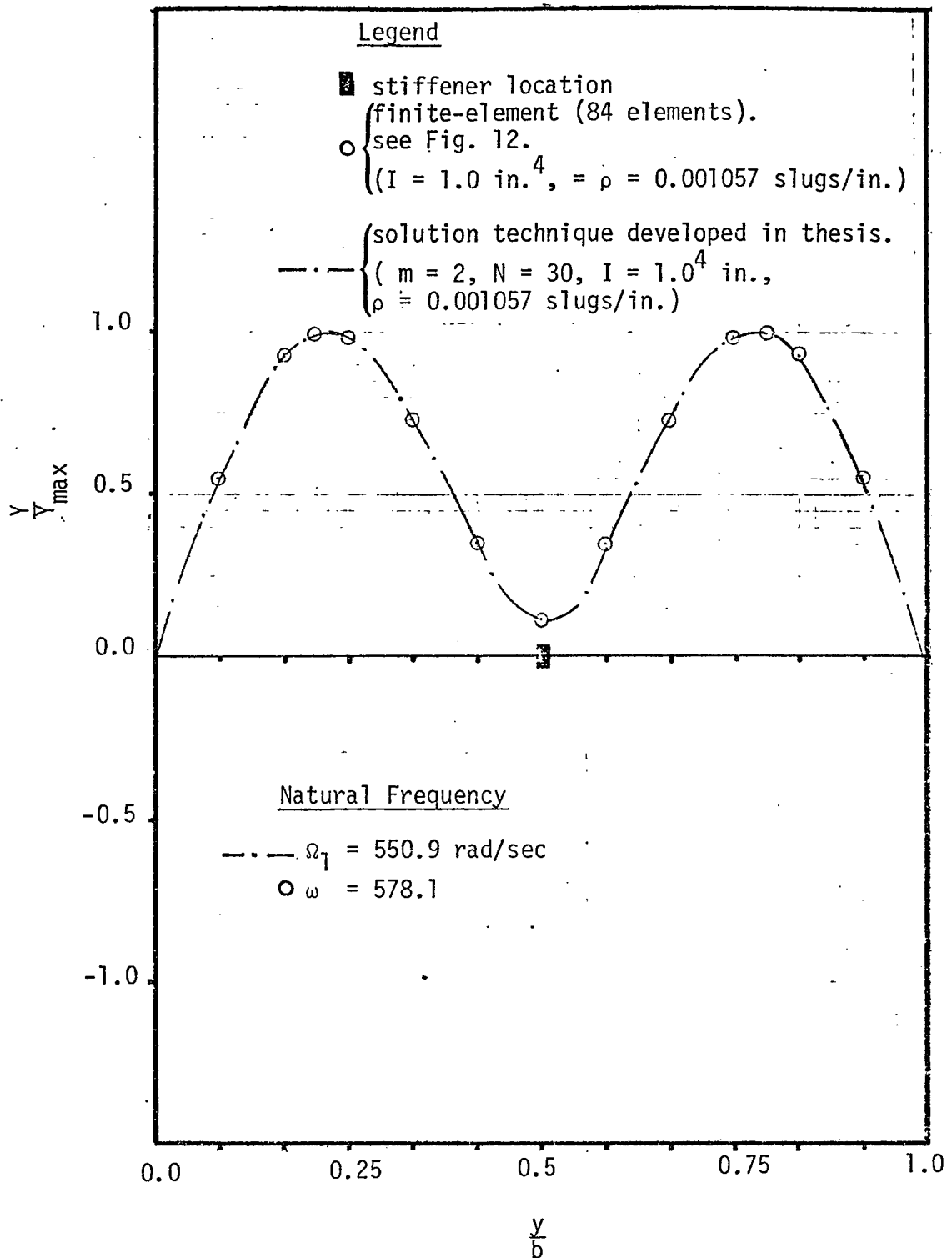


Fig. 14. Comparison of second lowest natural frequency and mode shape of Fig. 4 with finite-element solution.

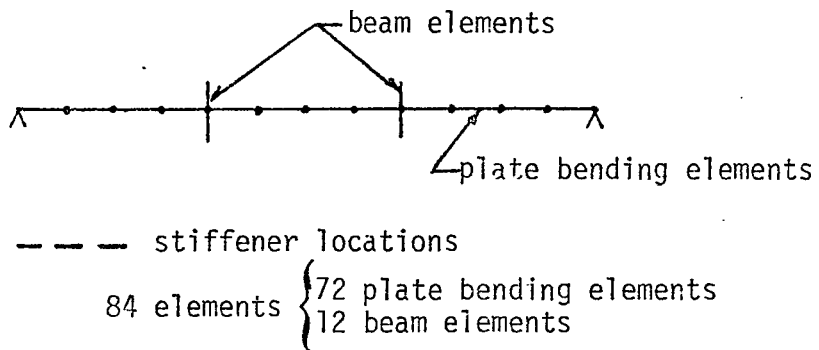
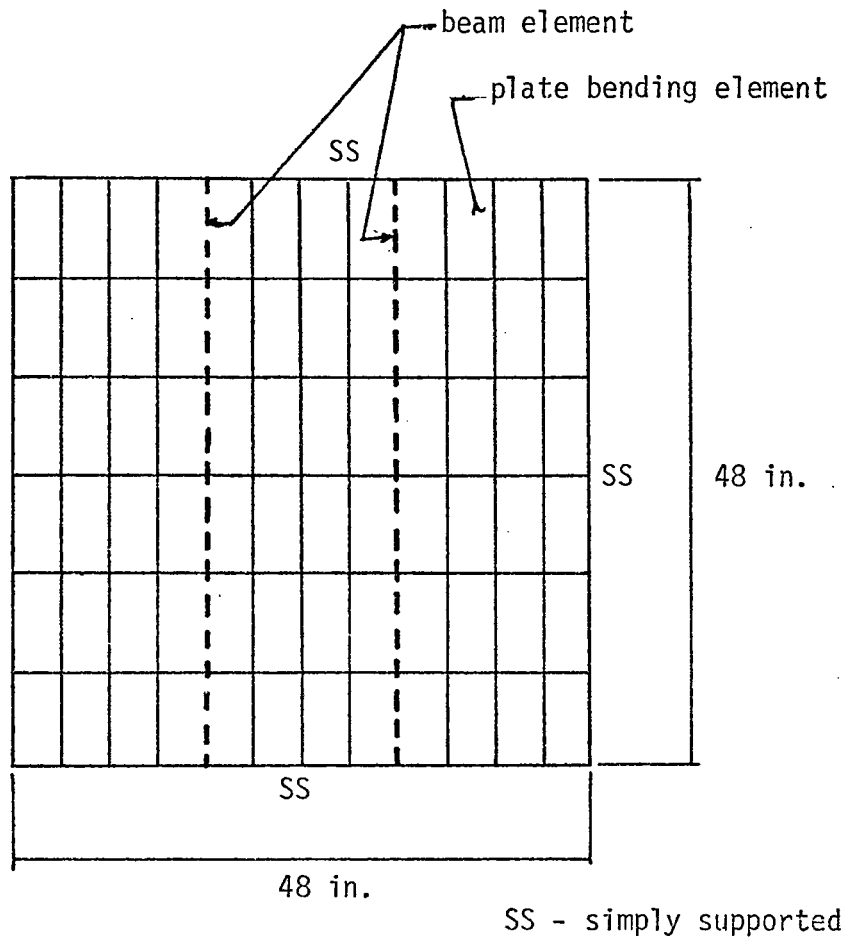


Fig. 15. Finite-element model for a square plate with two stiffeners.

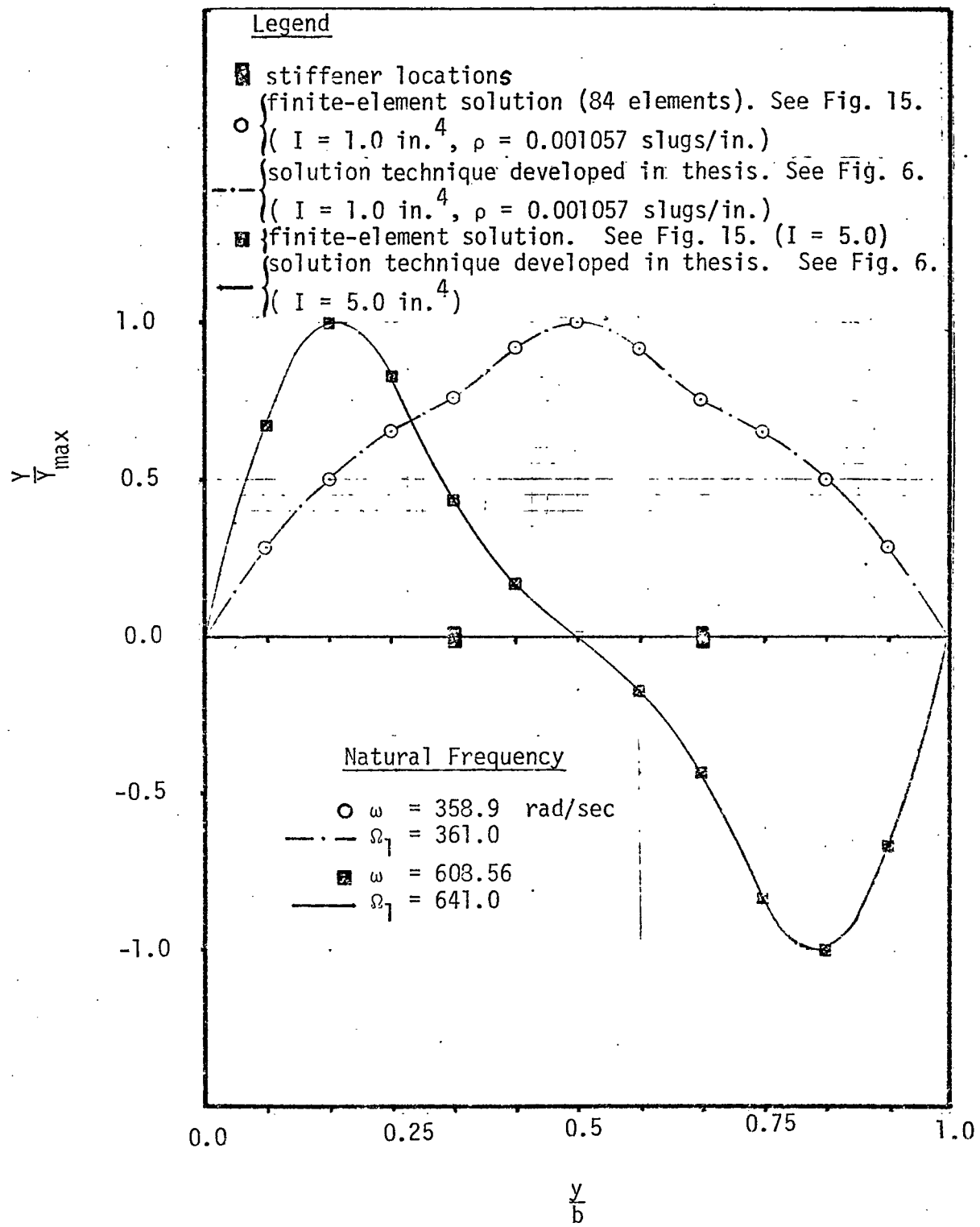


Fig. 16. Comparison of lowest (first) natural frequencies and mode shapes Fig. 6 with finite-element solutions.

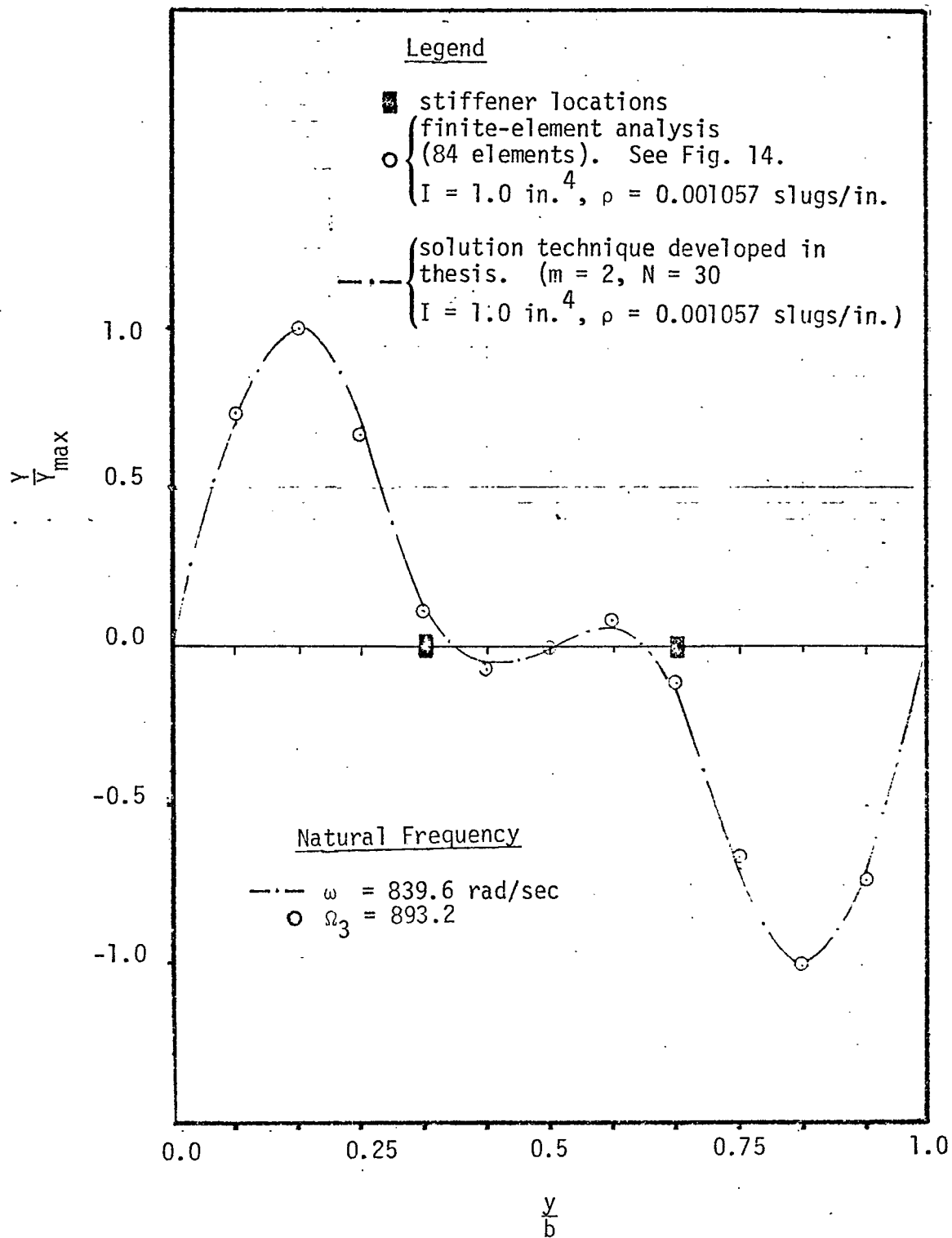


Fig. 17. Comparison of lowest (third) natural frequencies and mode shapes Fig. 8 with finite-element solution.

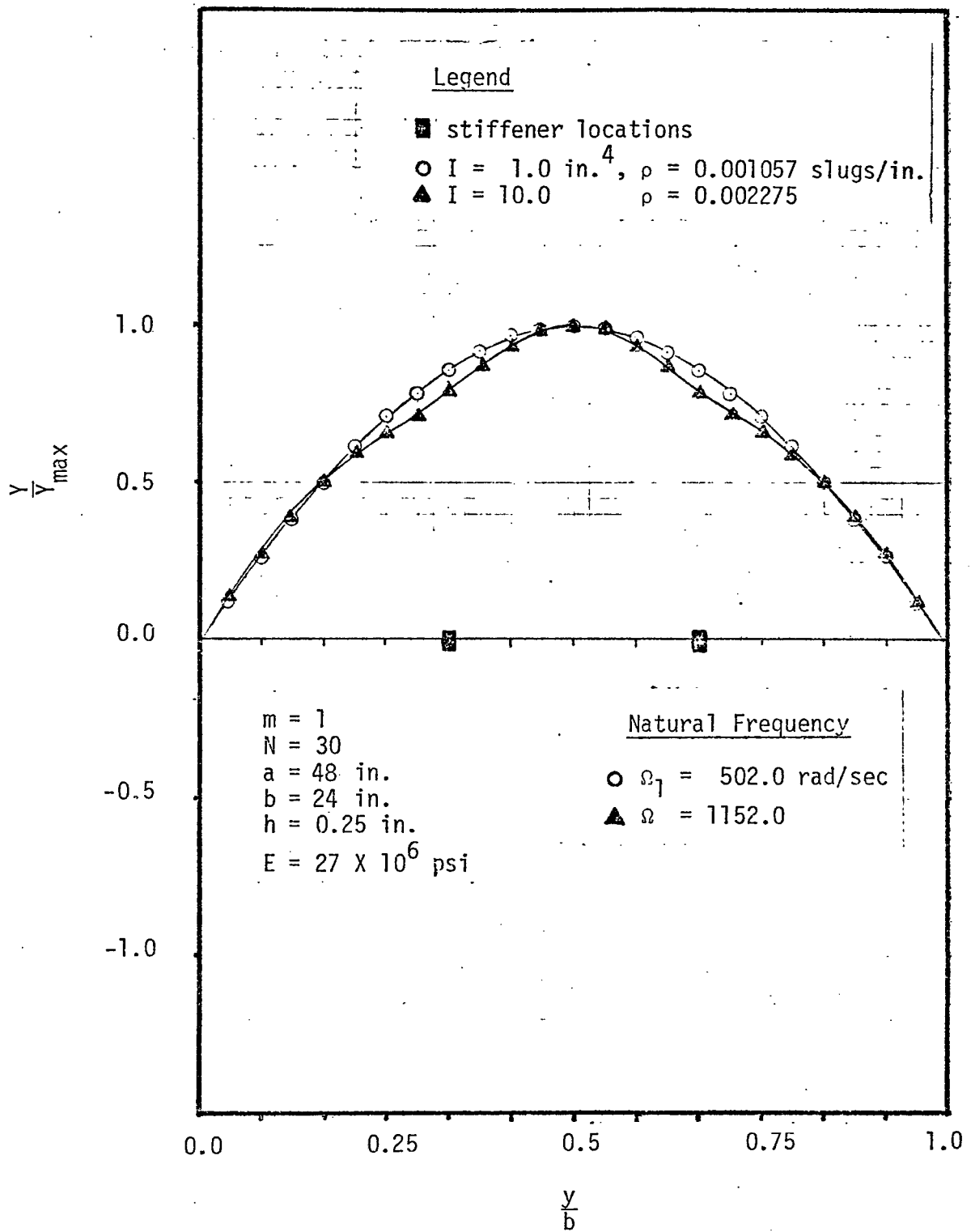


Fig. 18. Lowest (first) natural frequencies and mode shapes (at  $x/a = 0.5$ ) for a rectangular plate ( $a = 48 \text{ in.}$ ,  $b = 24 \text{ in.}$ ) with two stiffeners.

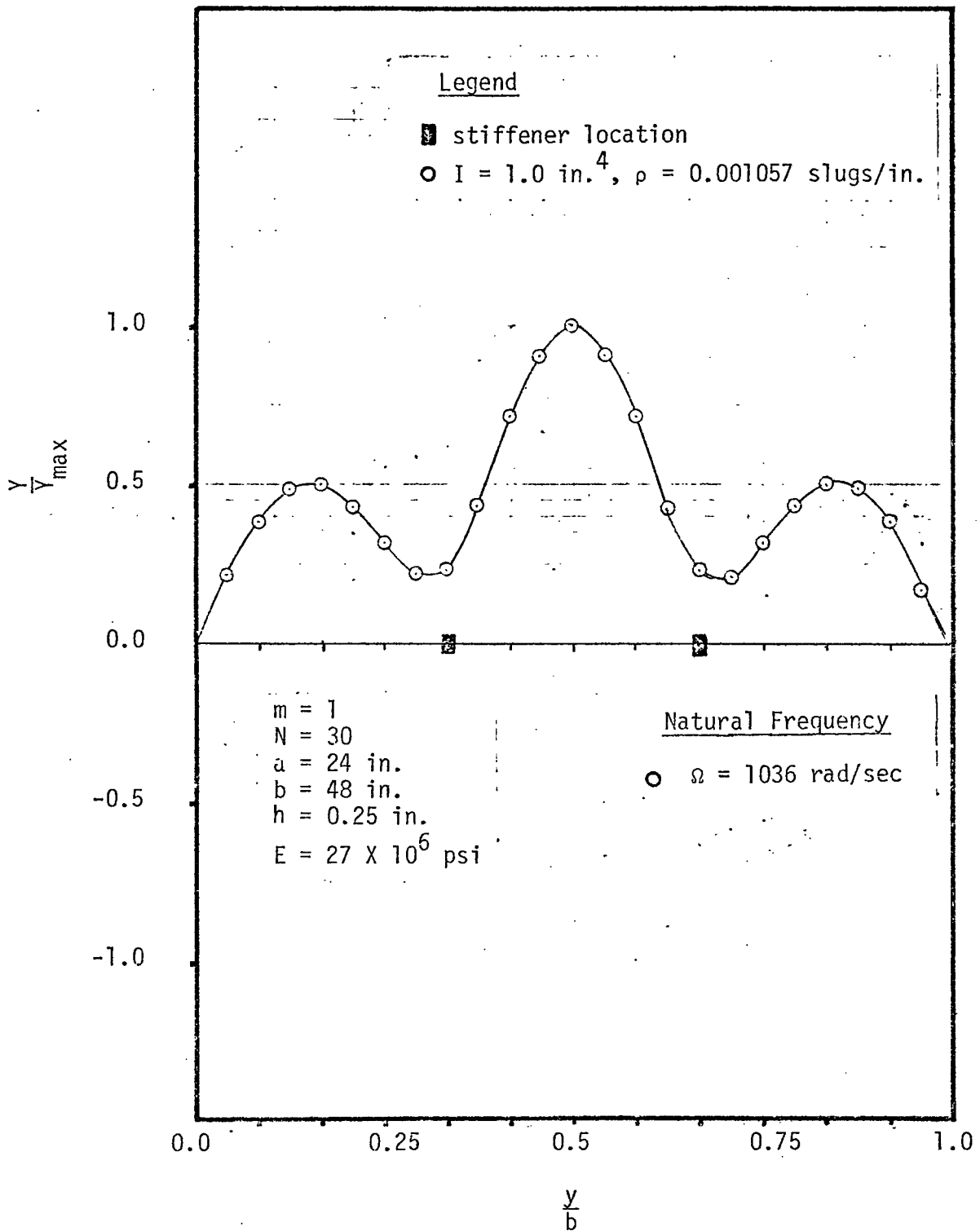


Fig. 19. Lowest (first) natural frequencies and mode shapes (at  $x/a = 0.5$ ) for a rectangular plate ( $a = 24 \text{ in.}$ ,  $b = 48 \text{ in.}$ ) with finite-element solution.

## CHAPTER V

### CONCLUSION AND RECOMMENDATIONS

From the results and comparisons presented in Chapter IV it is concluded that the method developed in this thesis is a very straight forward and accurate method of determining the natural frequencies and associated mode shapes for a plate with an arbitrary number of stiffeners. In particular for plates which are sparsely stiffened, and therefore, can not be treated by orthotropic plate theory, it establishes a very inexpensive analysis tool. Less than two cpu seconds were used in obtaining the first three natural frequencies and mode shapes given for each stiffened plate presented in cases (i), (ii) and (iii).

In conclusion, it is recommended to extend the work presented in this thesis in the following ways:

- (1) The torsional resistance of the stiffeners be incorporated into the analysis.
- (2) Consider stiffeners whose neutral-axis are not necessarily located at the mid surface of the plate.
- (3) Consider arbitrarily spaced stiffeners parallel to both the x-axis and y-axis.
- (4) The natural frequencies and associated mode shapes given by the methods of this thesis be used in a modal analysis to obtain the response to an arbitrary forcing function normal to stiffened plate's mid surface.

Also, experimental determination of the natural frequencies and mode shapes of a sparsely stiffened plate would be most useful to the analyst.

BIBLIOGRAPHY

1. Huffington, N. J., Jr. and Hoppmann, N. H., II, "On the Transverse Vibration of Rectangular Orthotropic Plates," Journal of Applied Mechanics, Vol. 25, 1958, pp. 389-395.
2. Hoppmann, W. H., II, and Magness, L. S., "Nodal Pattern of the Free Flexural Vibration of Stiffened Plate," Journal of Applied Mechanics, Vol. 24, 1957, pp. 526-530.
3. Huffington, N. J., Jr., "Theoretical Determination of Rigidity Properties of Orthogorally Stiffened Plates," Dissertation, The John Hopkins University, Baltimore, Md., 1954.
4. Timoshenko, S. and Woinowski-Krieger, S., Theory of Plates and Shells, 2nd Edition, McGraw-Hill, New York, 1959, pp. 111-113.
5. Lin, Y. K., "Free Vibration of Continuous Skin-Stringer Panels," Journal of Applied Mechanics, Vol. 27, 1960, pp. 669-676.
6. Irving, J. and Mullineau, N., "Rectangular Plates with Stringers and Ribs," Journal of the Aeronautical Sciences, Vol. 21, 1954, pp. 847-848.
7. Soler, A. I. and Afshari, H., "On the Analysis of Cable Network Vibrations Using Galerkin's Method," Journal of Applied Mechanics, Vol. 37, No. 3, 1970, pp. 607-611.
8. Michalopoulos, C. D. and Wheeler, L. T., "Deflection Analysis of Rectangular Plates Reinforced by Pre-Trained Stiffeners," Journal of Applied Mechanics, Vol. 42, Brief notes, 1975, pp. 901-903.
9. Hamming, R. W., Introduction to Applied Numerical Analysis, McGraw-Hill, New York, 1971, pp. 46-47.
10. McCormick, J. M. and Salvadori, M.G., Numerical Methods in Fortran, Prentice-Hall, Englewood Cliffs, New Jersey, 1964, pp. 71-73.

APPENDIX A



```

      WRITE(6,884)VALUE
884  FCFORMAT(SX,'VALUE=',E13.6)
      IF(K.EQ.1)GO TO 100
      IF(VALUE*VALUE1)70.7C,100
C
C   VALUE OF EXPANDED DETERMINANT IS NEGATIVE OF ZERO.
C
70  CCNTINUE
      VV=DABS(VALUE-VALUE1)
      IF(VV.GT.5.)GO TO 97
C
C
      CALL ROCTS(VALUE,VALUE1,FREQC,DELFREQ,FAC,CCC4,NSTIF,L,CK,
1  IFREQP,FRECB,IFREQ,XFREQ,CMAT)
C
C
100  IF(NSTIF.EQ.1) VALUE1=VALUE
      GO TO 501
97   WRITE(6,95)FREQC
95   FORMAT(SX,'***PCLE OF FREQ. EQ.(APPROX.)***',E13.6)
      IF(NSTIF.EQ.1)VALUE1=VALUE
C
C
501  CCNTINUE
      WRITE(6,997)
997  FCFORMAT(SX,'NATURAL FREQUENCY OF STIFFENED PLATE:',//)
      DO 998 I=1,IFREQ
          WRITE(6,999)I,XFREQ(I)
999  FORMAT(10X,'NATURAL FREQUENCY(',I,',')=',E13.6)
998  CCNTINUE
      RETURN
      END
C
C
C
C
C   SUBROUTINE EXPANDS DETERMINANT.
C
      SUBROUTINE DETEXP(C,NSTIF,VALUE)
C
      IMPLICIT REAL*8(A-H,O-Z)
C
      DIMENSION A(20,20),B(20,20),C(20,20)
      DO 150 I=1,NSTIF
          DO 150 J=1,NSTIF
              A(I,J)=C(I,J)
150  CCNTINUE
C
      NNN=NSTIF-1
      FACX=1.
      NNN=NSTIF-1
      NNN1=NSTIF-2
      DO 139 LL=1,NNNN
          TACX=CABS(FACX)
          IF(TACX.LT.1.0E-40) GO TO 510
          IF(TACX.GT.1.0E 40) GO TO 510
          GO TO 500
510  FACX=A(1,1)*FACX
          I=1
          DO 520 J=1,NNN
              A(1,J)=A(1,J)/A(1,1)
520  CCNTINUE
500  CONTINUE
          FACX=FACX/(A(1,1)*NNN1)
          WRITE(6,301)FACX
301  FCFORMAT(SX,E13.6)
          DO 140 J=1,NNN
              DO 140 I=1,NNN
                  B(I,J)=A(1,1)*A(I+1,J+1)-A(1,J+1)*A(I+1,1)
140  CCNTINUE

```



```

1120 CONTINUE
C
1800 CONTINUE
      RETURN
      END
      SUBROUTINE ROOTS(VALUE,VALUE1,FREOC,DELFRQ,FAC,CCC4,NSTIF,L,CK,
1FRECP,FRECB,IFREQ,XFREQ,CMAT)
C
      IMPLICIT REAL*8(A-H,C-Z)
      DIMENSION BD(99),Z(20,20),FREOP(99),C(20,20),CK(20),
1XFREQ(20),CMAT(20,400)
C
      ICOUNT=0
      FRECC1=FFREOC-DELFRQ
C
90 CCNTINUE
C
      FREQ1=(FRECC1*VALUE-FREOC*VALUE1)/(VALUE-VALUE1)
C
      DO 30 I=1,L
      FC(I)=FREOP(I)-FREQ1**2
30 CONTINUE
C
      EN=FRECB-FREQ1**2
C
      DO 49 I=1,NSTIF
      DO 50 II=1,NSTIF
      ZZ=0.
      DO 51 J=1,L
      Z(I,II)=ZZ+EN*DSIN(J*CCC4*CK(II))*DSIN(J*CCC4*CK(I))/BD(J)
      ZZ=Z(I,II)
51 CCNTINUE
      Z(I,II)=FAC*Z(I,II)
50 CONTINUE
49 CONTINUE
C
      PUT IN A FORM FOR THE EXPANSION OF THE DETERMINANT.
C
      DO 55 I=1,NSTIF
      C(I,I)=1.0+Z(I,I)
55 CCNTINUE
C
      DO 56 I=1,NSTIF
      DO 56 J=1,NSTIF
      IF(I.EQ.J)GO TO 53
      C(I,J)=Z(I,J)
53 CCNTINUE
56 CCNTINUE
C
      CALL SUBROUTINE TO EXPAND THE DETERMINANT.
C
      IF(NSTIF.EQ.1) GO TO 89
      CALL DETEXP(C,NSTIF,VALUEX)
      GO TO 401
89 VALLEX=C(1,1)
401 CONTINUE
C
      WRITE(6,400)VALLEX
400   FORMAT(5X,'VALUEX=',E13.6)
      VVV=DABS(VALUEX)
C
      ICOUNT=ICOUNT+1
      WRITE(6,299)ICOUNT
299   FORMAT(5X,'ICOUNT=',I2)
      IF(ICOUNT.GT.10)GO TO 79
      IF(VVV.LT..0000001)GO TO 79
C
      IF(VALUE1*VALUEX)75,75,77
C
75   FRECC=FREQ1
      VALUE=VALUEX
      VALUE1=VALUE1/2.0

```

```

      GO TO 90
C
C
77   FREQC1=FREQ01
      VALUE1=VALUEX
      VALUE=VALUE/2.0
      GO TO 90
C
C
79   IFREQ=IFREQ+1
      III=0
      DO 150 I1=1,NSTIF
      DO 150 J1=1,NSTIF
      III=III+1
      CMAT(IFREQ,III)=C(I1,J1)
209  WRITE(6,209)IFREQ,III,CMAT(IFREQ,III)
150  CONTINUE
C
      XFREQ(IFREQ)=FREQ01
      WRITE(6,720)FREQ01,VALUEX
720  FORMAT(5X,'ROOT FREQUENCY=',E13.6,/,5X,
1     'VALUE OF EXP. DET.',E13.6)
      RETURN
      END
C
C
C
C
      SUBROUTINE VECTOR(NSTIF,CMAT,IFREQ,YD)
      IMPLICIT REAL*8(A-H,C-Z)
      DIMENSION C(20,20),B(20,20),YD(20,20),CMAT(20,400)
C
      DO 105 KK=1,IFREQ
      WRITE(6,300)KK
C
      II=0
      DO 150 I1=1,NSTIF
      DO 150 J1=1,NSTIF
      II=II+1
      C(I1,J1)=CMAT(KK,II)
      WRITE(6,209)C(I1,J1)
209  FORMAT(5X,'C=',E13.6)
150  CONTINUE
C
      DO 110 K=1,NSTIF
      IJ=NSTIF+K
      DO 101 I=1,NSTIF
      DO 100 J=1,NSTIF
C
      IF(I.EQ.NSTIF)GO TO 100
      IF(J.EQ.K)GO TO 109
      IF(ISKIP.EQ.1)GO TO 120
C
      E(I,J)=C(I,J)
      GO TO 100
C
120  CONTINUE
      E(I,J-1)=C(I,J)
      GO TO 100
109  ISKIP=1
100  CONTINUE
      ISKIP=0
101  CONTINUE
      IF(NSTIF.NE.1) GO TO 249
      YD(KK,K)=1.0
      GO TO 251
249  IF(NSTIF.EQ.2)GO TO 250
      KNN=NSTIF-1

```

```

C
C
IF(MODE.EQ.1)GO TO 2030
CALL VECTOR(NSTIF,CMAT,IFREQ,Y0)
C
2020 CALL YMODE(XFREQ ,FRECP,FREOB,RHO,XU,B,NSTIF,DELY,
1CK,L,IFREQ,Y0)
C
2030 CONTINUE
STOP
END
C
C
C
C
SUBROUTINE FREQN( FREOB,FREOP,START,DELFRO,NN,B,RHO,XU,CK,
1L,NSTIF,VALUEX,VALUE, IFREQ,XFREQ,CMAT)
C
IMPLICIT REAL*8(A-H,C-Z)
DIMENSION FREOP(99),BC(99),Z(20,20),C(20,20),CK(20),XFREQ(20),
1CMAT(20,400)
C
FAC=2.0*RHO/(B*XU)
CCC4=3.141592654/B
IFREQ=0
C
DO 501 K=1,NN
FREOC=K*DELFRO+START
EN=FREQB-FREOC**2
C
DO 30 I=1,L
FU(I)=FREOP(I)-FREOC**2
30 CONTINUE
C
DO 49 I=1,NSTIF
DO 50 II=1,NSTIF
ZZ=0.
DO 51 J=1,L
Z(I,II)=ZZ+EN*DSIN(J*CCC4*CK(II))*DSIN(J*CCC4*CK(I))/BD(J)
ZZ=Z(I,II)
51 CONTINUE
Z(I,II)=FAC*Z(I,II)
50 CONTINUE
49 CONTINUE
C
PUT IN FORM FOR THE EXPANSION OF THE DETERMINANT.
DO 55 I=1,NSTIF
C(I,I)=1.0+Z(I,I)
55 CONTINUE
C
DO 56 I=1,NSTIF
DO 56 J=1,NSTIF
IF(I.EQ.J)GO TO 53
C(I,J)=Z(I,J)
53 CONTINUE
56 CONTINUE
C
CALL SUBROUTINE TO EXPAND DETERMINANT.
C
IF(NSTIF.NE.1) GO TO 50
VALUE=C(1,1)
GO TO 89
90 IF(K.EQ.1) GO TO 88
VALUE1=VALUE
88 CONTINUE
CALL DETEXP(C,NSTIF,VALUE)
C
89 CONTINUE

```

```
C
C CALLS SUBROUTINE TO EXPAND DETERMINANT.
C CALL DETEXP(B,NNN,VALUE)
C COFACTORS OF DETERMINANT.
  YD(KK,K)=(-1.0)**IJ*VALUE
  GO TO 251
250  YD(KK,K)=(-1.0)**IJ*C(1,J-K)
251 CONTINUE
C
  WRITE(6,301)K,YD(KK,K)
300  FORMAT(5X,'MODAL VECTOR FOR',I2,' NATURAL FREQUENCY:',/)
301  FORMAT(10X,'Y(',I2,')=',E13.6)
C
110 CONTINUE
105 CONTINUE
  RETURN
  END
```